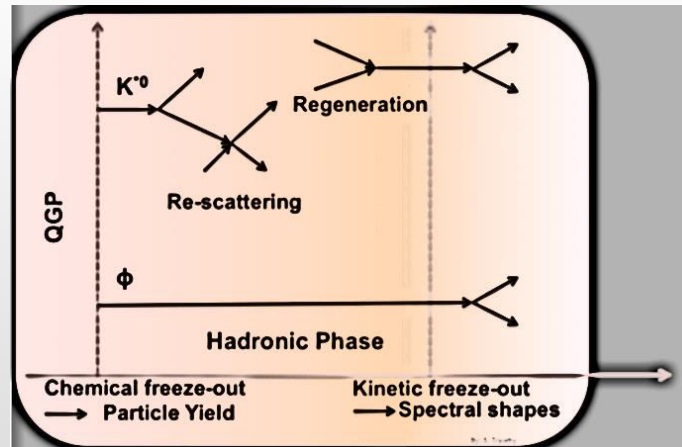


# Resonance production in heavy-ion collisions

V. Riabov



# Outline ...

- The world of resonances and corresponding physics observables is huge ...
- This contribution is limited to discussion of light-flavor ( $u, d, s$ ) hadronic resonances
- Review of experimental situation and basic predictions for resonance properties in heavy-ion collisions at different energies
- MPD capabilities to measure resonances

# Introduction

- Resonances are excited hadronic states with short lifetimes comparable to lifetime of the system produced in heavy-ion collisions
- Study of resonance properties in vacuum is not a subject of interest
- Instead, resonances are used as probes of the medium (partonic or hadronic) produced in heavy-ion collisions
- Modification of the reconstructed resonance properties in heavy-ion collisions carries information about the time evolution and conditions in the interacting system (temperature, density, degrees of freedom, etc.)
- Additional information can be inferred from comparison of the resonance properties measured in hadronic and leptonic decay channels, daughter hadrons participate in strong interactions with the surrounding QCD matter, while it is transparent for leptons

# Resonances

- A huge variety of resonances is known, listed in the Particle Data Group, [https://pdg.lbl.gov/2020/listings/contents\\_listings.html](https://pdg.lbl.gov/2020/listings/contents_listings.html)
- A small number of resonances has been studied the heavy-ion collisions:
  - ✓ well-defined reference → well-known vacuum properties (mass, width/lifetime, decay channels and branching ratios, quark content etc.)
  - ✓ produced at high rates in hadronic interactions at GeV-energies → experimentally measurable in high-multiplicity environment
  - ✓ do not have partners with similar masses → discernable from other particles

# Resonance candidates for measurements

- The most-often measured resonances

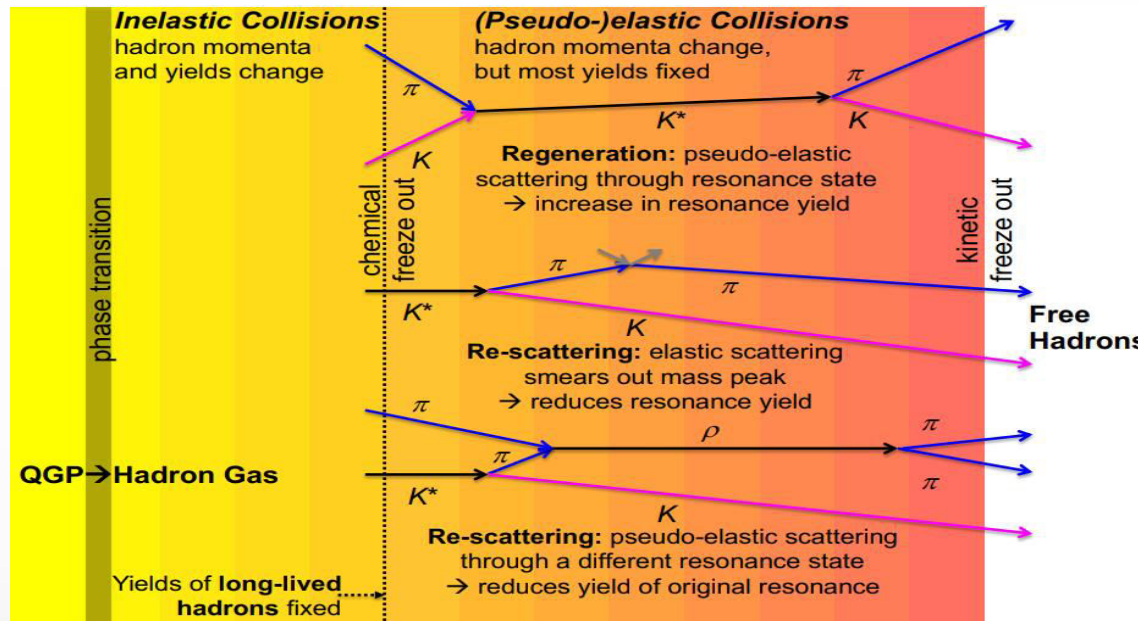


Particle	Mass (MeV/c <sup>2</sup> )	Width (MeV/c <sup>2</sup> )	Decay	BR (%)
$\rho^0$	770	150	$\pi^+\pi^-$	100
$K^{*+}$	892	50.3	$\pi^+K_s^-$	33.3
$K^{*0}$	896	47.3	$\pi^+K^+$	66.7
$\phi$	1019	4.27	$K^+K^-$	48.9
$\Sigma^{*+}$	1383	36	$\pi^+\Lambda$	87
$\Sigma^{*-}$	1387	39.4	$\pi^-\Lambda$	87
$\Lambda(1520)$	1520	15.7	$K^-\rho$	22.5
$\Xi^{*0}$	1532	9.1	$\pi^+\Xi^-$	66.7

- Can not be measured directly (short lifetimes, neutral particles) → invariant mass method
- Different masses, strangeness content → not unique to resonances
- Wide range of lifetimes (1-45 fm/c) → unique feature of resonances
- Probe reaction dynamics and particle production mechanisms:
  - ✓ density and lifetime of the hadronic phase
  - ✓ strangeness enhancement at high multiplicities
  - ✓ spin alignment
  - ✓ baryon enhancement and hadronization mechanisms, parton energy loss, etc.

# Resonances as probes of the hadronic phase

# Resonances in the hadronic phase



- Resonances provide the means to directly probe the hadronic phase properties
- Reconstructed resonance yields in heavy ion collisions are defined by:

- ✓ resonance yields at chemical freeze-out
- ✓ hadronic processes between chemical and kinetic freeze-outs:

**rescattering**: daughter particles undergo elastic scattering or pseudo-elastic scattering through a different resonance  $\rightarrow$  parent particle is not reconstructed  $\rightarrow$  loss of signal

**regeneration**: pseudo-elastic scattering of decay products ( $\pi K \rightarrow K^{*0}$ ,  $KK \rightarrow \phi$  etc.)  $\rightarrow$  increased yields

# Resonances as probes of the hadronic phase

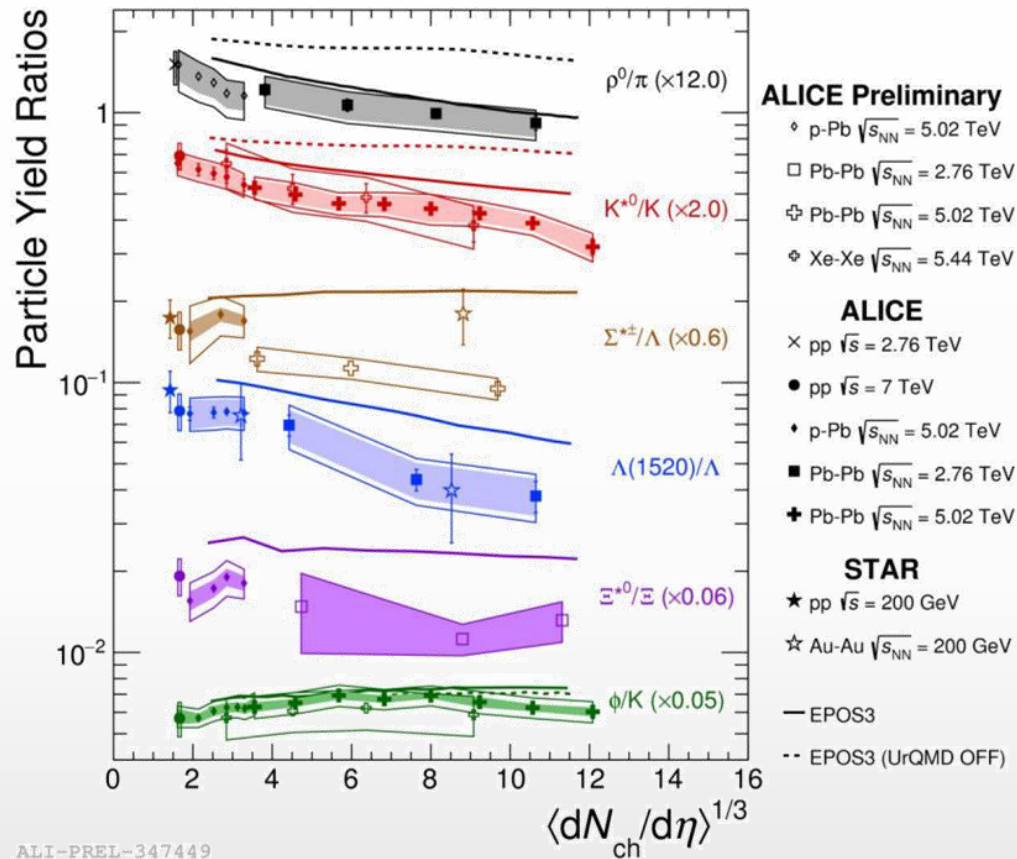
- Cumulative effect of the hadronic phase effects for resonances depends on:
  - ✓ lifetime and density of the hadronic phase
  - ✓ resonance lifetime and scattering cross sections (type of daughter particles)
- Resonances with lifetimes comparable to that of the fireball are well suited to study properties of the hadronic phase

	$\rho(770)$	$K^*(892)$	$\Sigma(1385)$	$\Lambda(1520)$	$\Xi(1530)$	$\phi(1020)$
$c\tau$ (fm/c)	1.3	4.2	5.5	12.7	21.7	46.2
$\sigma_{\text{rescatt}}$	$\sigma_{\pi}\sigma_{\pi}$	$\sigma_{\pi}\sigma_K$	$\sigma_{\pi}\sigma_{\Lambda}$	$\sigma_K\sigma_p$	$\sigma_{\pi}\sigma_{\Xi}$	$\sigma_K\sigma_K$

- Properties of the hadronic phase are studied by measuring the ratios of the resonance yields ( $p_T$ -integrated) to the yields of long-lived particles with similar quark contents:  $\rho(770)^0/\pi$ ,  $K^*(892)/K$ ,  $\phi(1020)/K$ ,  $\Lambda(1520)/\Lambda$ ,  $\Sigma(1385)^{\pm}/\Sigma$  and  $\Xi(1530)^0/\Xi$
- The ratios are measured as a function of the final state charged-particle multiplicity in pp (reference system), p-A (intermediate) and A+A (heavy-ion) collisions. The variation of the ratios with multiplicity probes the interplay between the rescattering and regeneration effects in the hadronic phase



# Experimental results, A+A at $\sqrt{s_{NN}} = 0.2-5$ TeV



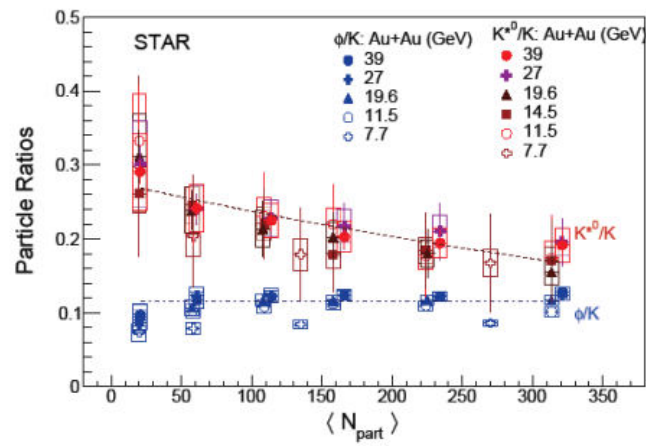
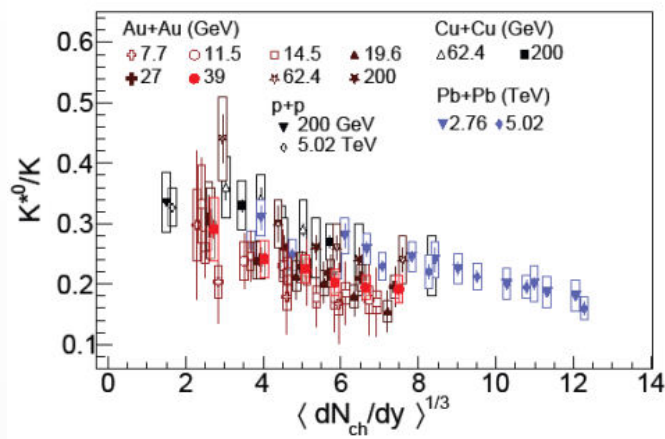
- Suppressed production of short-lived resonances ( $\tau < 20$  fm/c) in central A+A collisions  $\rightarrow$  rescattering takes over the regeneration
- No modification is observed for  $\phi$ -meson ( $\tau \sim 40$  fm/c)  $\rightarrow$  behaves like a stable particle
- Resonances with intermediate lifetimes show transition from suppression to no effect
- Yield modifications depend on event multiplicity, not on collision system/energy

▪ Results are qualitatively reproduced by EPOS3 + UrQMD

▪ Results support the existence of a hadronic phase that lives long enough ( $\tau \sim 10$  fm/c) to cause a significant reduction of the reconstructed yields of short-lived resonances

# What about NICA energies?

- First results available from STAR BES program → consistent within large uncertainties

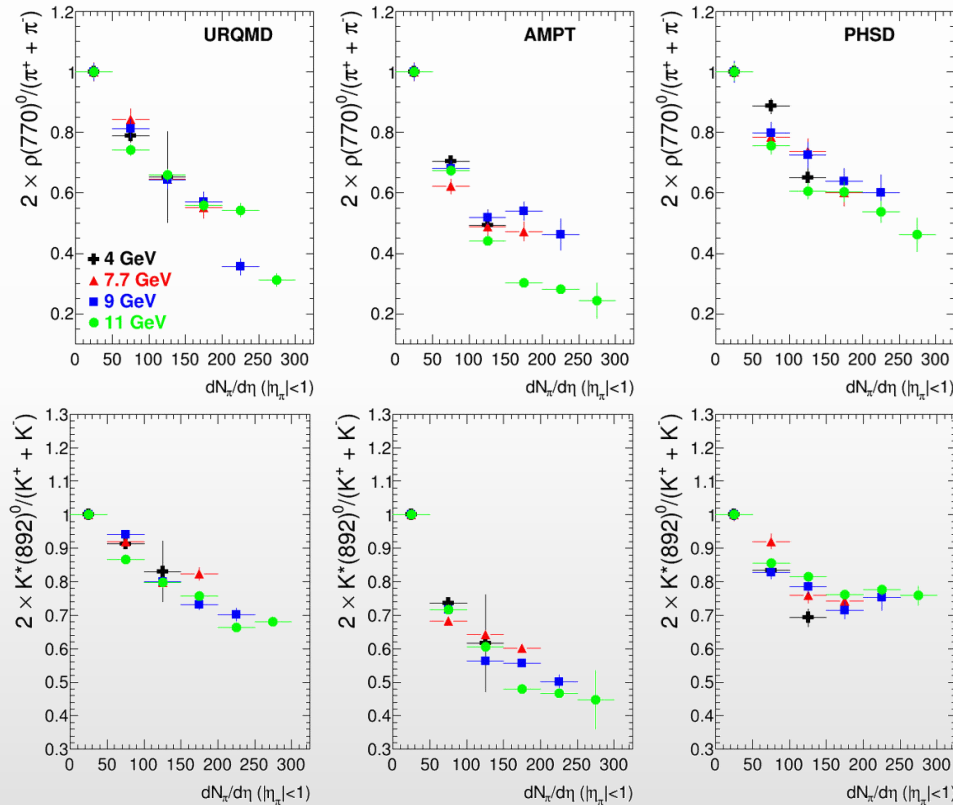


- Use model predictions: UrQMD, PHSD, AMPT event generators with hadronic cascades
- Resonances are decayed by the generators, final state particles in the output files
- Resonance yields can be estimated by accumulating invariant mass distributions for different combinations of daughter particles, integrating peaks from decays of the resonances in the distributions and correcting them for the branching ratios
- The whole procedure resembles what is done for the resonance reconstruction in real data analyses only with ideal particle identification and 100% detector efficiency

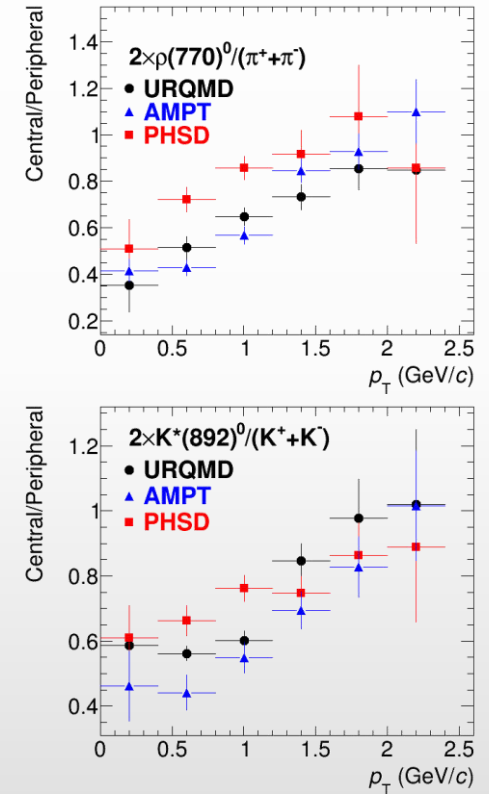
# Au+Au at $\sqrt{s_{NN}} = 4-11$ GeV: $\rho/\pi$ , $K^*/K$

- UrQMD, PHSD, AMPT event generators with hadronic cascades
- Ratios are shown normalized to most peripheral collisions  $\rightarrow$  start at unity at low multiplicity

Au+Au @ 4, 7.7, 9 and 11 GeV, ratios vs. multiplicity



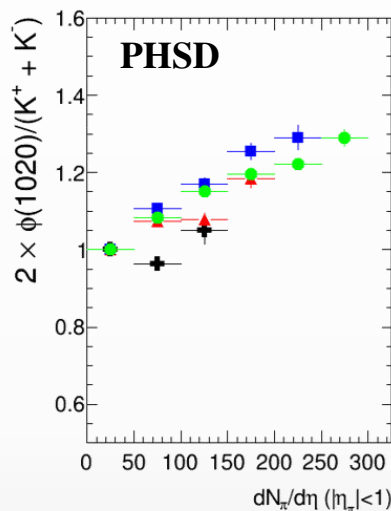
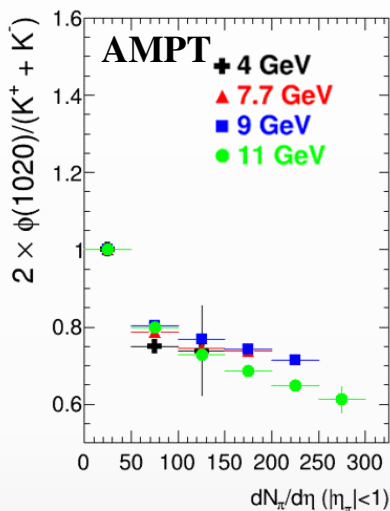
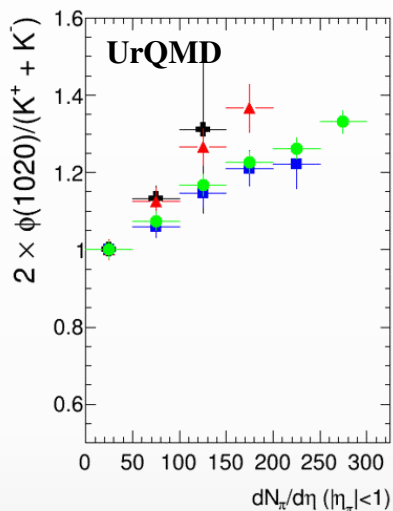
Au+Au @ 11 GeV, ratios vs.  $p_T$



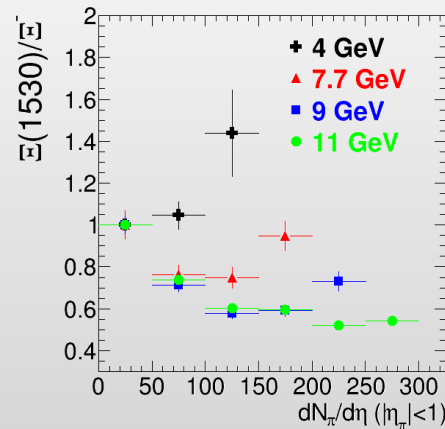
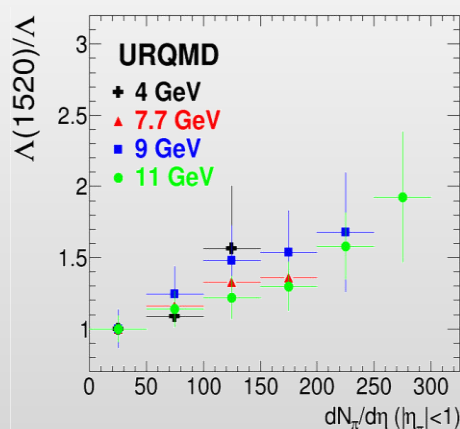
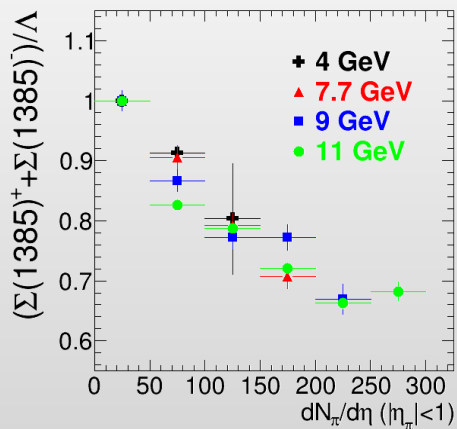
- models predict suppression of  $\rho/\pi$  and  $K^*/K$  ratios in Au+Au@4-11, resonances with small  $\tau$
- suppression depends on the final state multiplicity rather than on collision energy
- modifications occur at low momentum as expected for the hadronic phase effects

# Au+Au at $\sqrt{s_{NN}} = 4-11$ GeV: $\phi/K$ , $\Sigma^*/\Lambda$ , $\Lambda^*/\Lambda$ , etc.

- UrQMD, PHSD, AMPT event generators with hadronic cascades
- Ratios are shown normalized to most peripheral collisions  $\rightarrow$  start at unity at low multiplicity

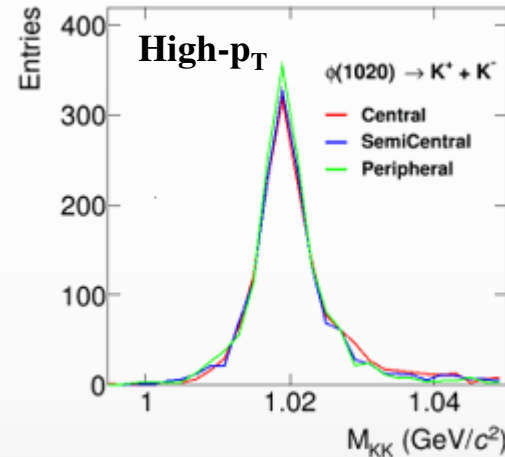
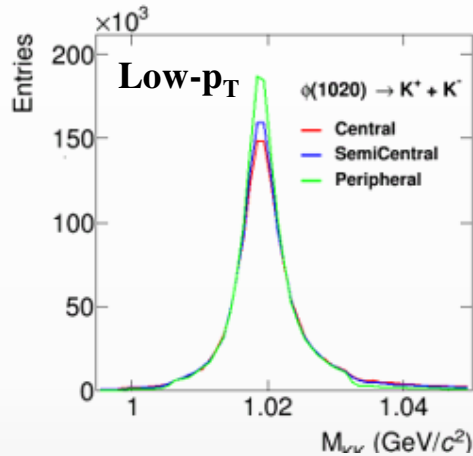


- $\phi(1020)/K$  ratio is predicted to be enhanced by UrQMD and PHSD and suppressed by AMPT
- $\Lambda(1520)/\Lambda$  ratio gradually increases,  $\Sigma(1385)^\pm/\Lambda$  and  $\Xi(1530)/\Xi^-$  decrease with multiplicity at all energies
- ratios are consistent for different collision energies at similar multiplicities

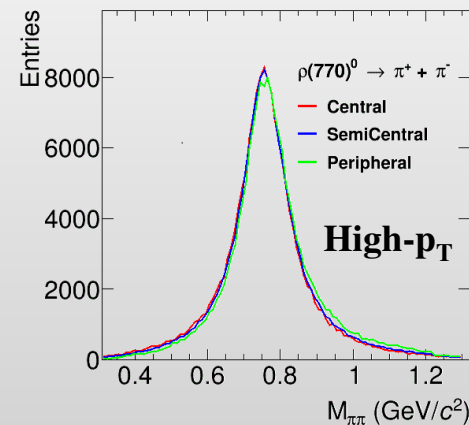
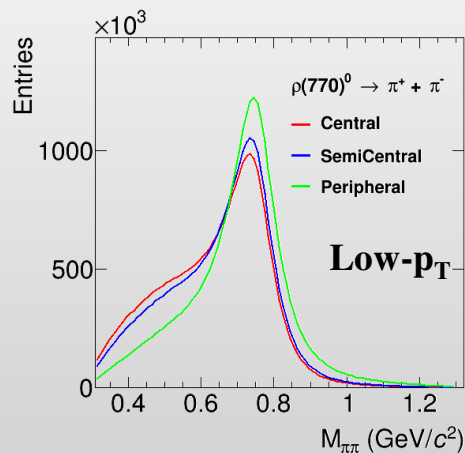


# Resonances in AuAu@11, UrQMD

- Resonances are decayed by UrQMD, daughters participate in elastic and inelastic scattering
- Resonance are reconstructed by invariant mass method, true daughters in the final state are used
- $\phi \rightarrow K^+K^-$  ( $c\tau \sim 45$  fm/c): modest line shape modifications in central AuAu@11 at low  $p_T$

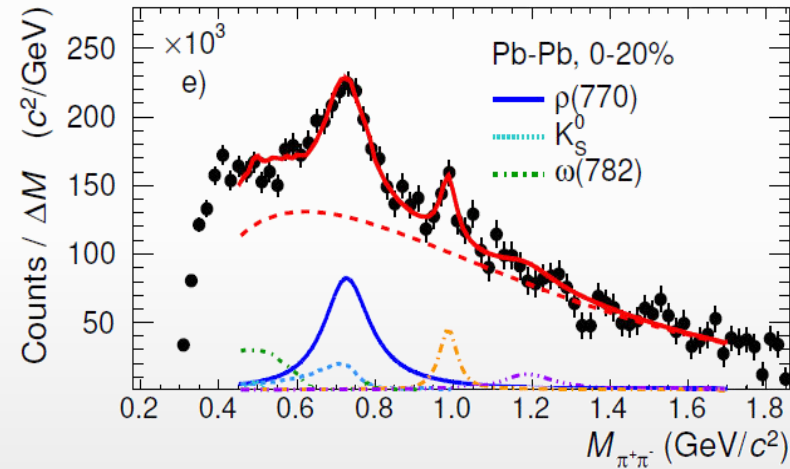
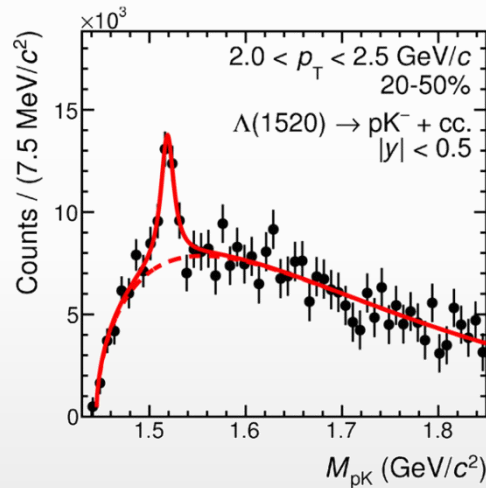
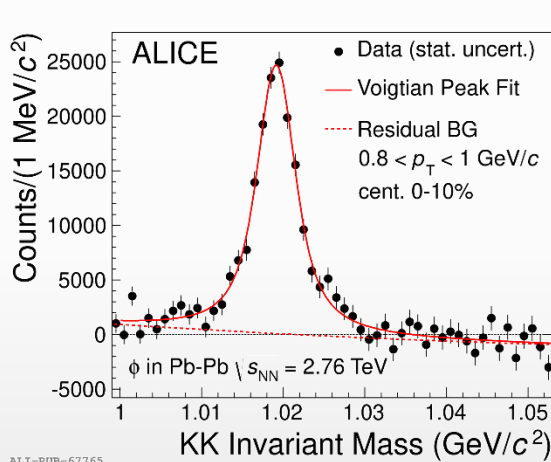


- $\rho(770)^0 \rightarrow \pi^+\pi^-$  ( $c\tau \sim 1.3$  fm/c): significant line shape modifications in central AuAu@11 at low  $p_T$



# Resonance reconstruction in A-A collisions

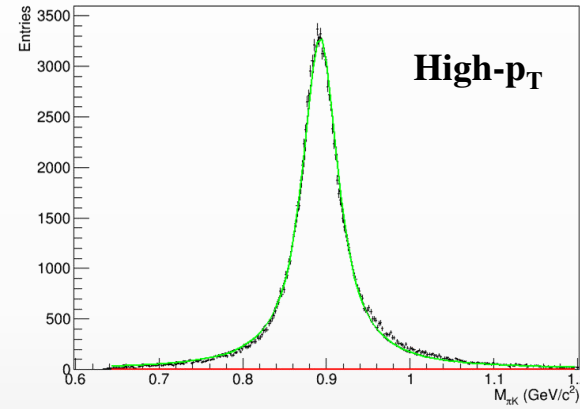
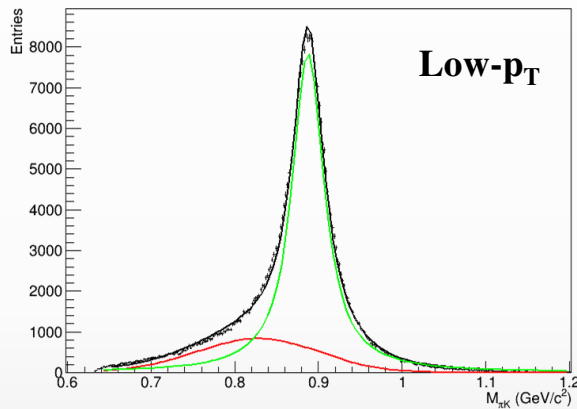
- Hadronic decays of resonances are studied with the invariant mass method in the experiments
- After subtraction of uncorrelated combinatorial background estimated with mixed-event pairs, like-sigh pairs, rotation pairs etc., the resonance peaks are approximated with a given peak-model (rBW + mass resolution + mass-dependent width + phase space correction + ...) + background function
- Examples of invariant mass distributions and fits from ALICE for  $\phi$ ,  $\Lambda(1520)$  and  $\rho(770)^0$ :



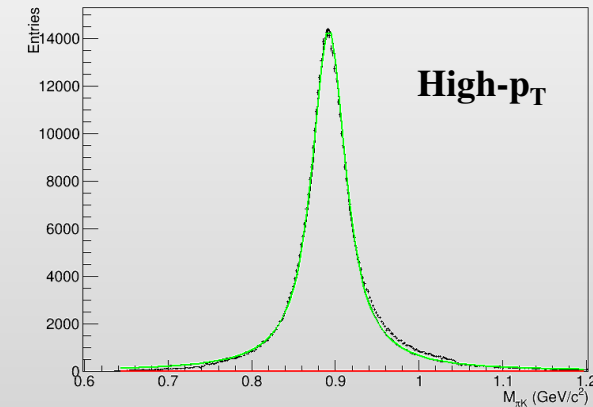
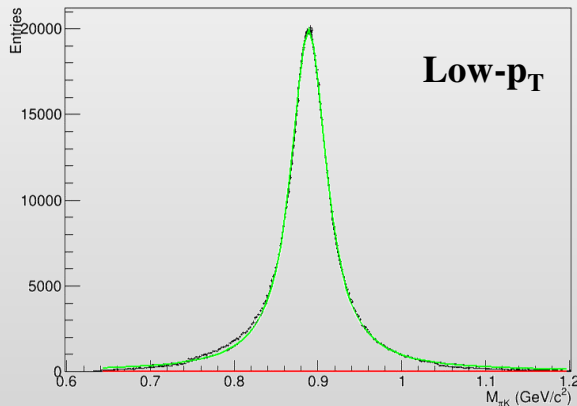
- For most of the cases, extraction of peak shapes from the measured invariant distributions is not possible  $\rightarrow$  peak models are inspired by theory and measurements in elementary  $e^+e^-$  and/or  $pp$  collisions where medium effects are not as important
- Possible line shape modifications will eventually result in the change of the measured yield and masses/widths when analyzed/fit with vacuum shapes

# Yield and mass modifications in AuAu@11

- UrQMD, AuAu@11 GeV,  $|y| < 1$
- $K^*(892)^0 \rightarrow \pi^\pm K^\pm$  ( $c\tau \sim 4.2$  fm/c); combine  $\pi^\pm K^\pm$  pairs from true  $K^*(892)^0$  decays
- Same fitting function for  $K^*(892)^0$  and background as in ALICE
- Central collisions: small line shape modifications at low  $p_T$ ; nothing at higher momentum

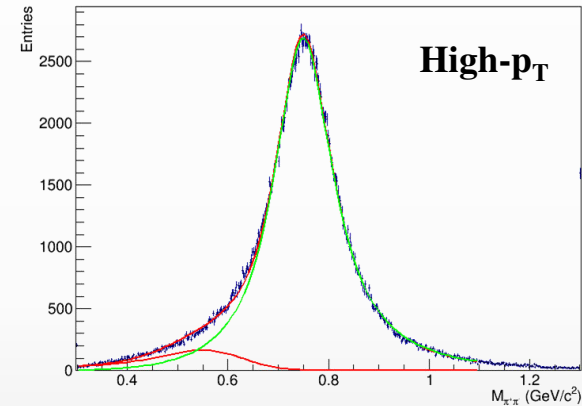
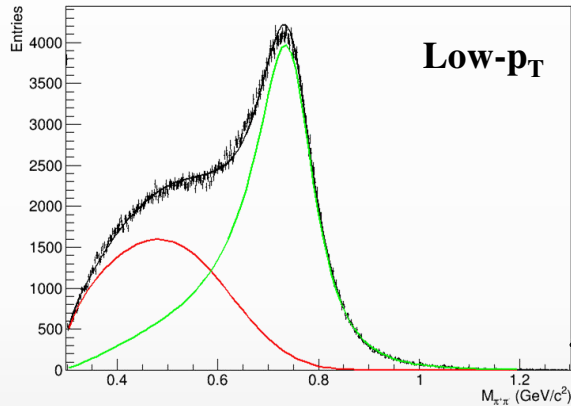


- Peripheral collisions: nothing

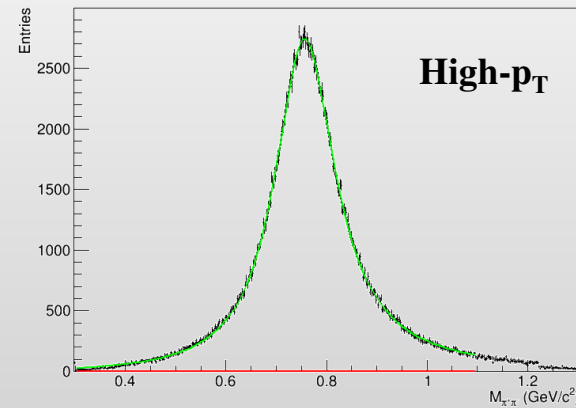
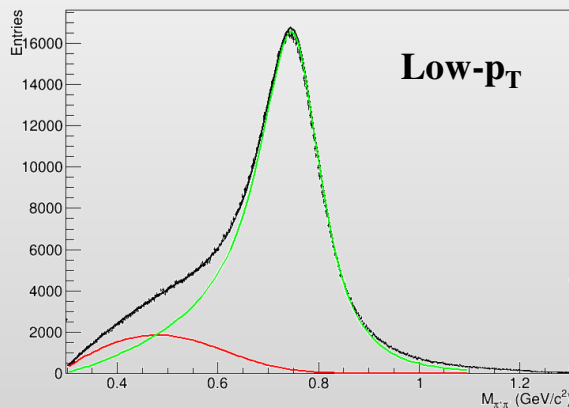


# Yield and mass modifications in AuAu@11

- $\rho(770)^0 \rightarrow \pi^+\pi^-$  ( $c\tau \sim 1.3$  fm/c); combine  $\pi^+\pi^-$  pairs from true  $\rho(770)^0$  decays
- Same fitting function for  $\rho(770)^0$  and background as in ALICE
- Central collisions: significant line shape modifications; excess with respect to the peak model is ascribed to background function



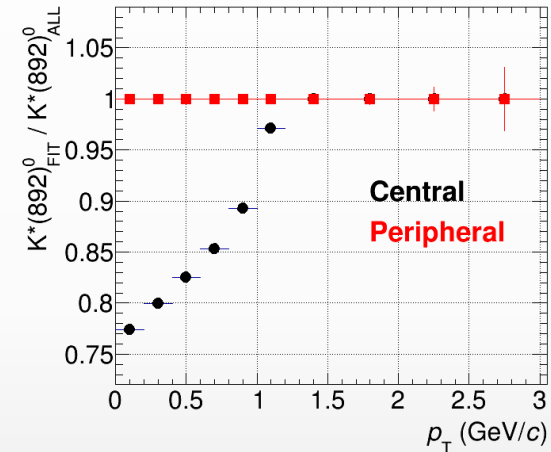
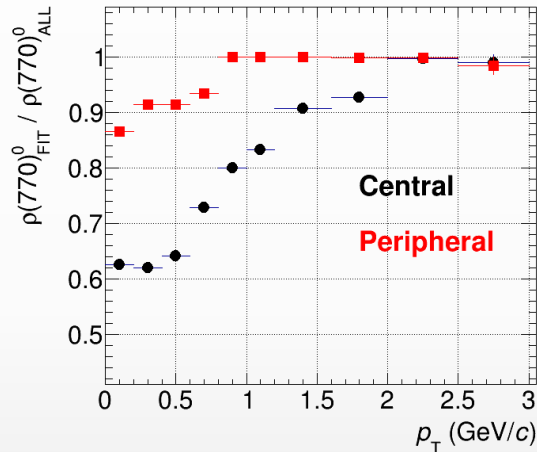
- Peripheral collisions: much smaller modifications are observed, only at low momentum





# Yields of $K^*(892)^0$ and $\rho(770)^0$ in AuAu@11

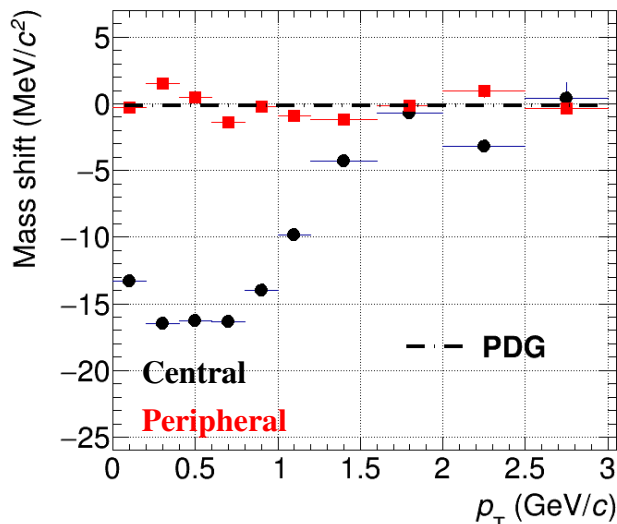
- Fraction of the true yield accounted for by the vacuum peak shape (the rest is assigned to background)
- ❖  $\rho(770)^0 \rightarrow \pi^+\pi^-$  ( $c\tau \sim 1.3$  fm/c)
  - ✓ yield is undercounted because of pion rescattering;
- ❖  $K^*(892)^0 \rightarrow \pi^\pm K^\pm$  ( $c\tau \sim 4.3$  fm/c)
  - ✓ yield is undercounted because of pion and kaon rescattering



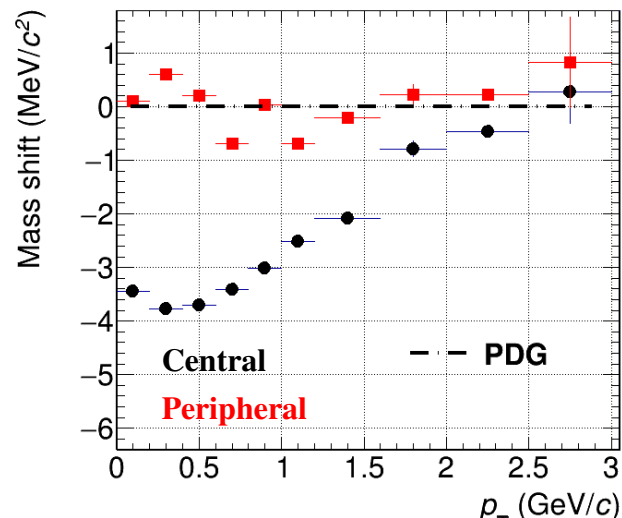
- Signal losses are larger for shorter-lived  $\rho(770)^0 \rightarrow$  higher chance for  $\rho(770)^0$  to decay and for daughters to rescatter in the medium
- Predicted signal losses are noticeable for the total ( $p_T$ -integrated) yields since bulk of the hadrons is produced at low  $p_T$  at NICA energies

# Masses of $K^*(892)^0$ and $\rho(770)^0$ in AuAu@11

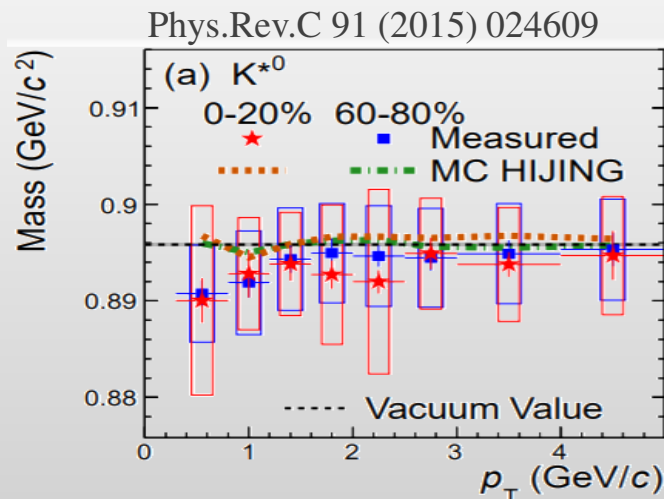
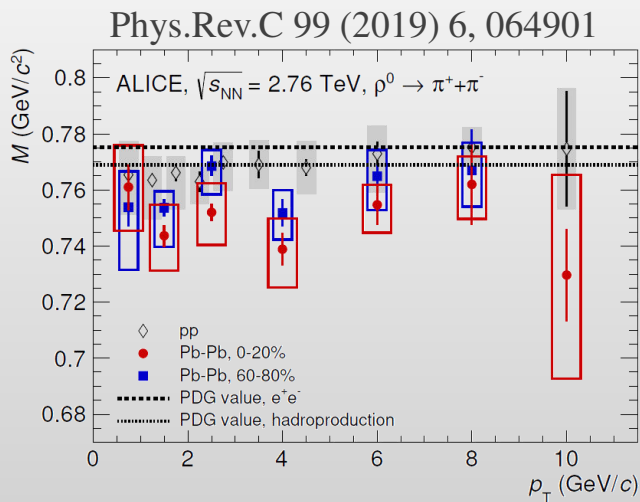
❖  $\rho(770)^0 \rightarrow \pi^+\pi^-$  ( $c\tau \sim 1.3$  fm/c)



❖  $K^*(892)^0 \rightarrow \pi^\pm K^\pm$  ( $c\tau \sim 4.3$  fm/c)



- In peripheral collisions, the peak models return masses and widths as measured in vacuum
- In central collisions, the masses are measured smaller
- Similar mass “modifications” have been reported @ RHIC and the LHC, large uncertainties:



# Summary for lower energies, $\sqrt{s_{NN}} = 4-11 \text{ GeV}$

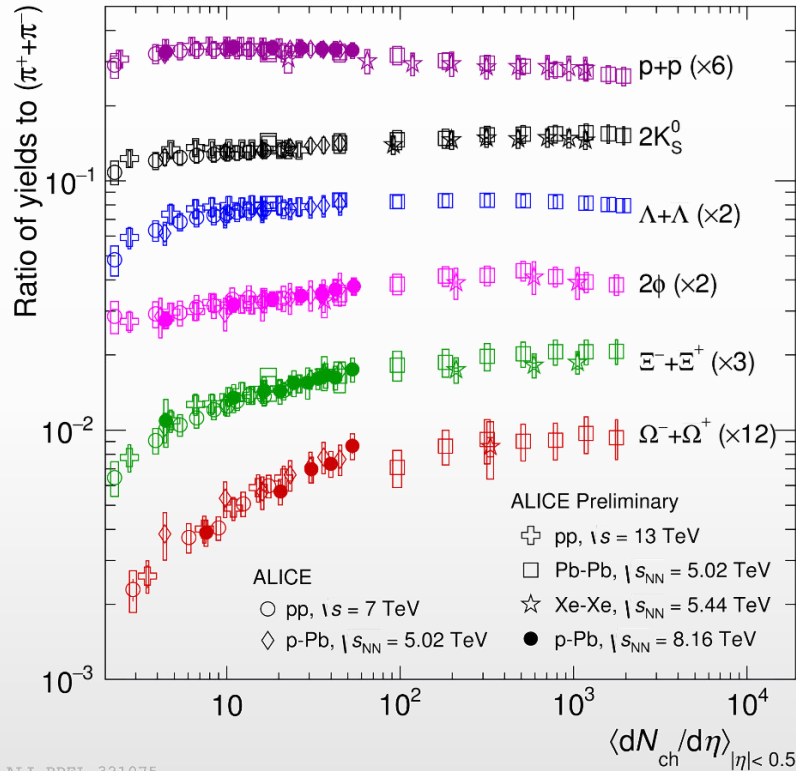
- Models predict yield modifications for resonances at NICA energies
- Modifications are qualitatively similar to those experimentally observed at RHIC/LHC:
  - ✓ lifetime and density of the hadronic phase are high enough
  - ✓ modification of particle properties in the hadronic phase should be taken into account when model predictions for different observables are compared to data
  - ✓ study of short-lived resonances is a unique tool to tune the hadronic phase simulations

# Strangeness enhancement and spin alignment

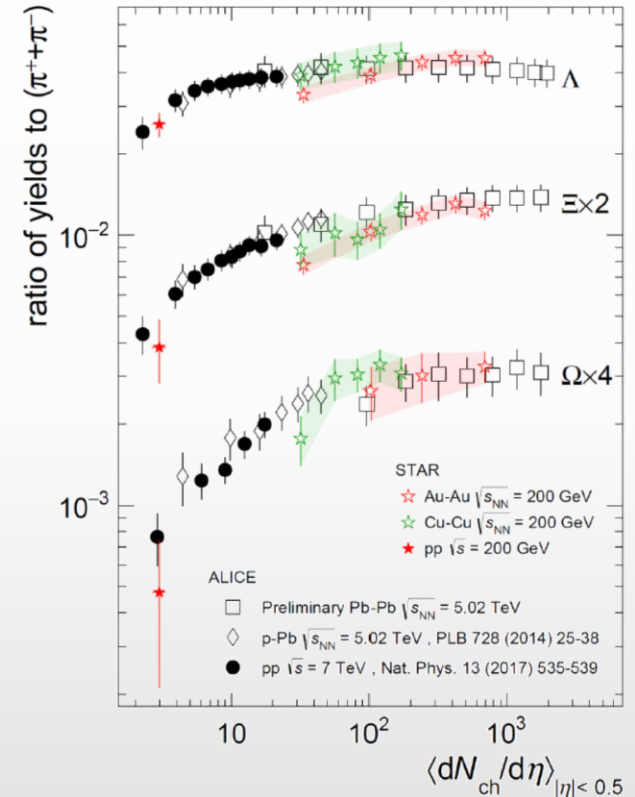
# Strangeness production: pp, p-A, A-A

- ❖ Since the mid 80s, strangeness enhancement is considered as a signature of the QGP formation
- ❖ Experimentally observed in heavy-ion collisions at AGS, SPS, RHIC and LHC energies

Nature Phys. 13 (2017) 535



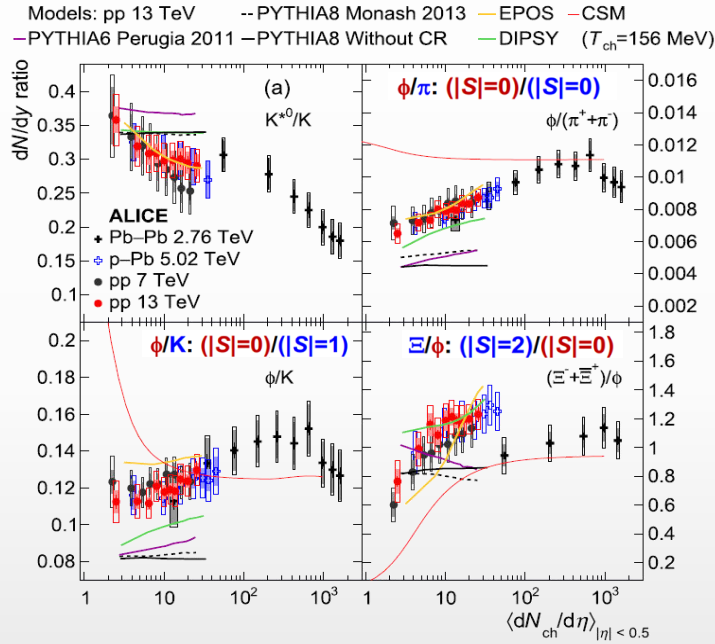
$|S| = 0$   
 $|S| = 1$   
 $|S| = 1$   
 $|S| = 0$  (hidden)  
 $|S| = 2$   
 $|S| = 3$



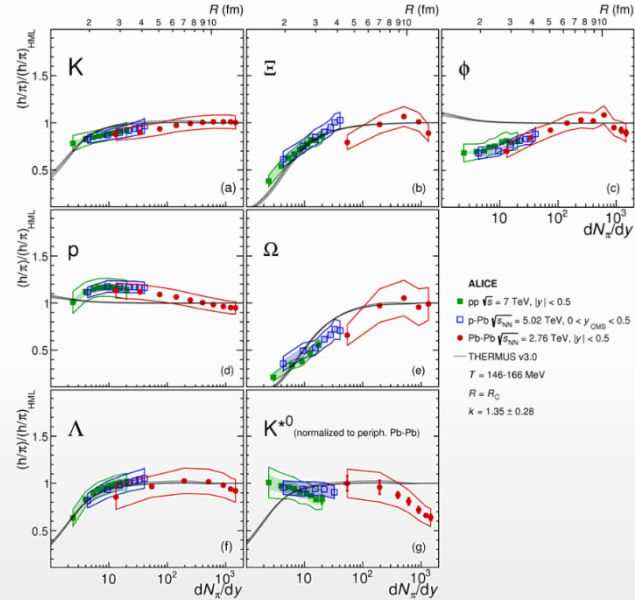
- ❖ Smooth evolution vs. multiplicity in pp, p-A and A-A collisions at LHC energies
- ❖ Strangeness enhancement increases with strangeness content and particle multiplicity
- ❖ STAR @ RHIC measurements in pp, A-A are in agreement with ALICE @ LHC at similar  $\langle dN_{ch}/d\eta \rangle$

- Origin of the strangeness enhancement in small/large systems is still under debate:
  - ✓ strangeness enhancement in QGP contradicts with the observed collision energy dependence
  - ✓ strangeness suppression in pp within canonical suppression models reproduces most of results except for  $\phi(1020)$

Phys. Lett. B807 135501(2020)



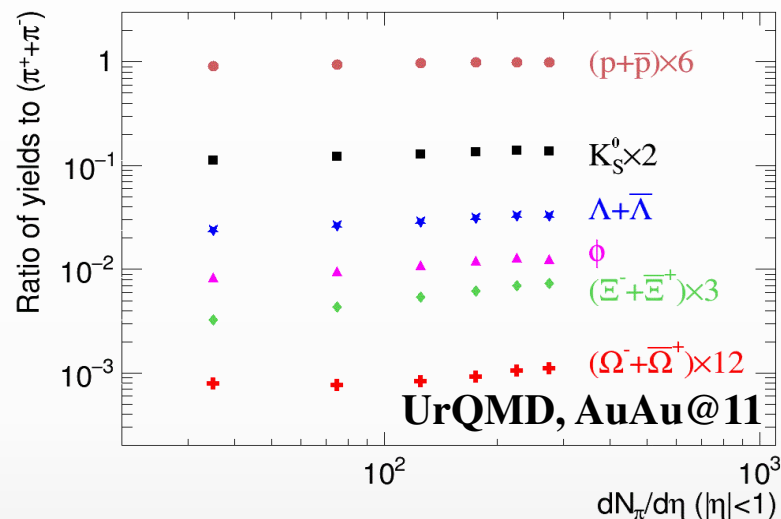
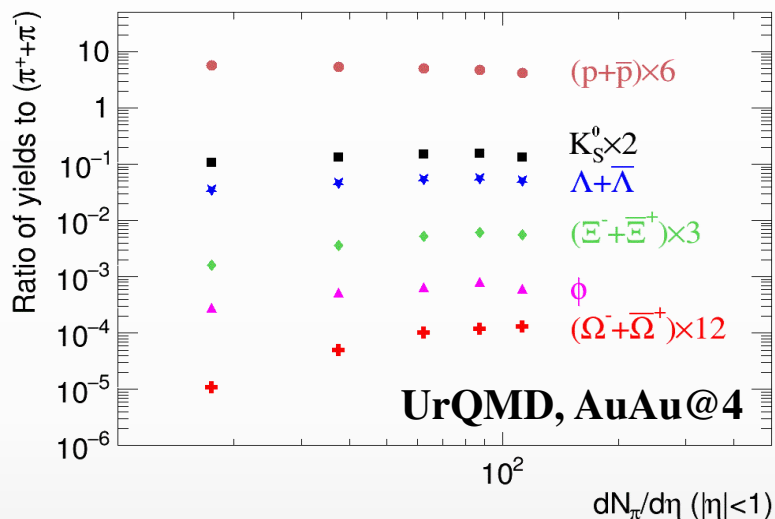
V. Vislavicius, A. Kalweit, arXiv:1610.03001



- $\phi$  with hidden strangeness is a key probe to study strangeness enhancement
  - ✓  $\phi/\pi$  increases with multiplicity in pp/p-Pb  $\rightarrow$  not expected for canonical suppression
  - ✓  $\phi/\pi$  saturates in Pb-Pb and is consistent with thermal model predictions
- Ratios  $\phi/K$  and  $\Xi/\phi$  show weak dependence on multiplicity  $\rightarrow$  has an effective strangeness of 1-2
- Origin of the strangeness enhancement in small/large systems is still debated

# Strangeness enhancement at lower energies, $\sqrt{s_{NN}} = 4-11$ GeV

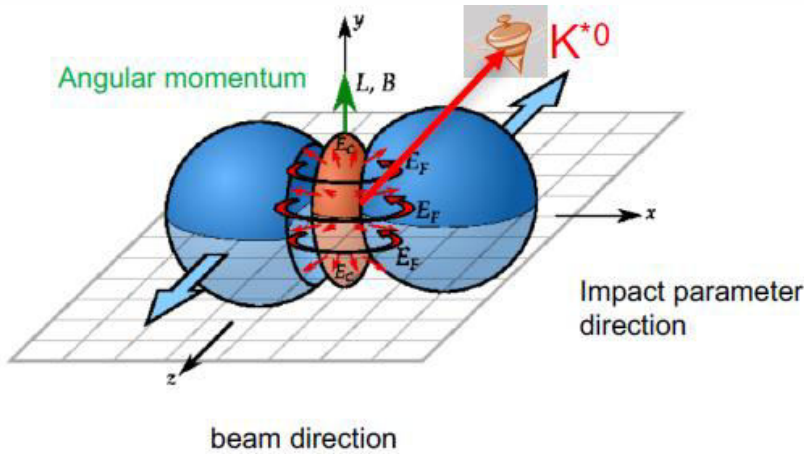
- Predictions of the event generators: UrQMD, PHSD, AMPT, EPOS ...
- ✓ models predict enhanced production of particles with strangeness, for example UrQMD:



- ✓ predictions of other event generators are qualitatively similar
- ✓ enhancement is more pronounced for particles containing a larger number of s-quarks
- ✓ relative enhancement is stronger at lower collision energies
- ✓  $\phi(1020)$  meson (a key observable) behaves like a hadron with open strangeness

- System size scan at NICA energies is needed

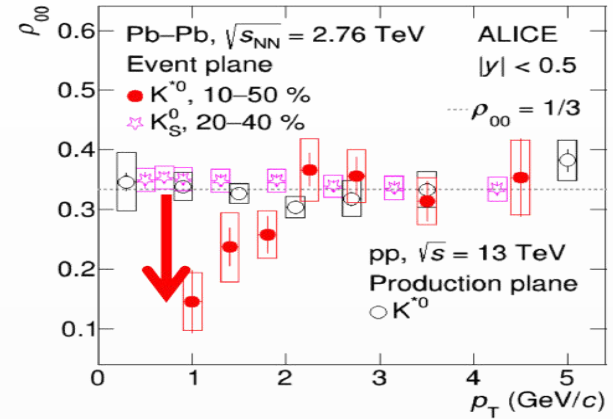
# Spin alignment of vector mesons in rotating QGP



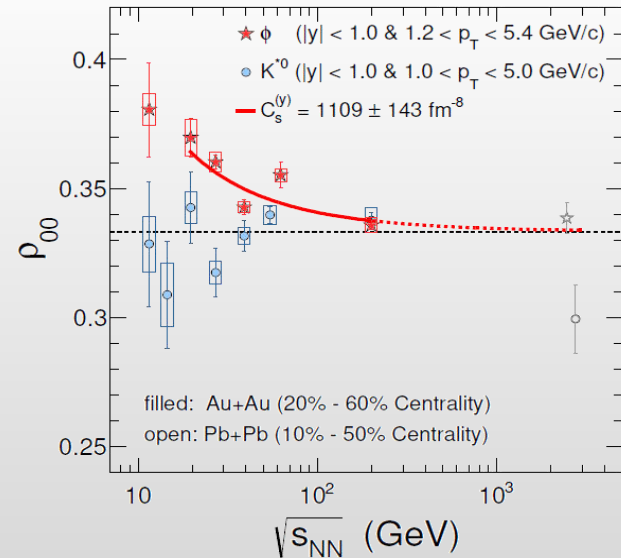
$$\frac{dN}{d\cos\theta} = N_0 [1 - \rho_{0,0} + \cos^2\theta (3\rho_{0,0} - 1)]$$

$\rho_{0,0}$  is a probability for vector meson to be in spin state = 0

- Large angular momentum  $L$  in non-central collisions  $\rightarrow$  *rotating QGP* ( $\sim 10^{21}$  revolutions per second)
- Spin-orbit interactions expect to polarize quarks
- If *vector mesons* (spin = 1) are produced as a result of quark recombination, the *spin alignment* can occur
- Complimentary measurement to hyperon global polarization



Measurements of  $K^*(892)^0 \rightarrow \pi K$  with respect to the event plane have shown a ***3 $\sigma$  effect at low momentum*** in Run-I

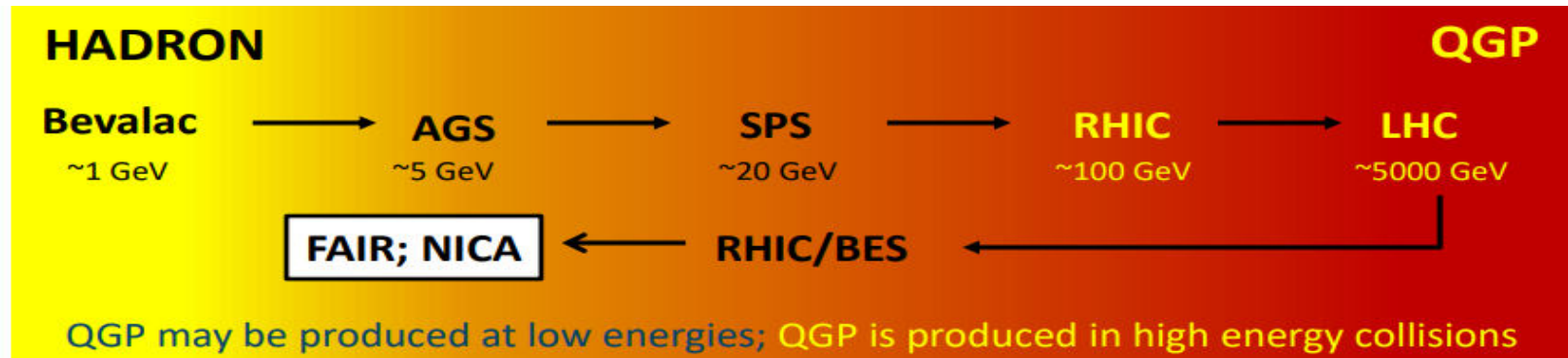


STAR & ALICE are consistent when analyzed in the same kinematical ranges

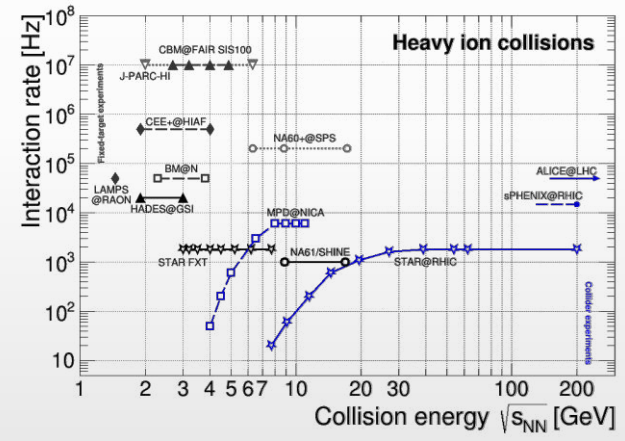
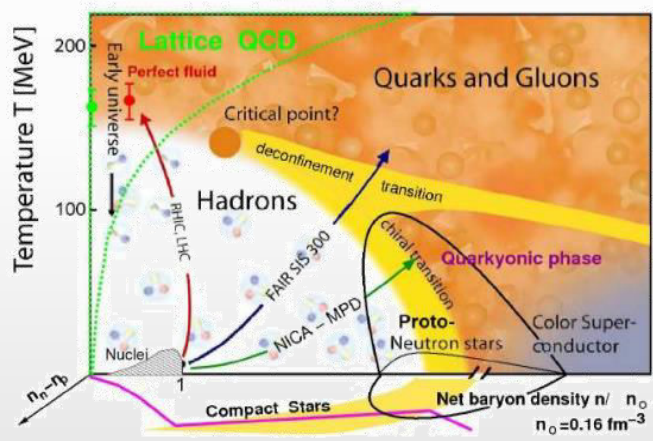


# Resonances with MPD@NICA

# Heavy-ion collisions



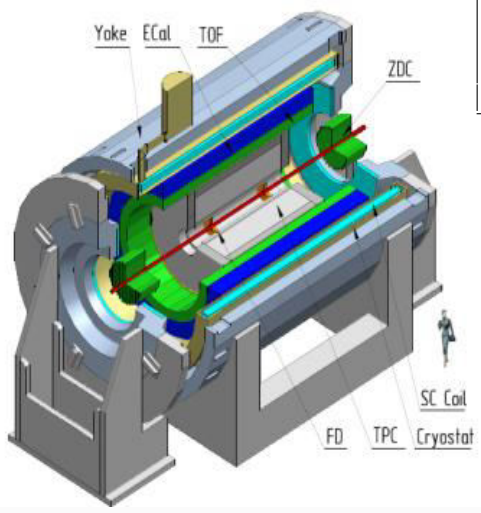
[https://github.com/tgalatyuk/interaction\\_rate\\_facilities](https://github.com/tgalatyuk/interaction_rate_facilities)



- Study of the QCD medium at extreme net baryon densities, phase transition at  $\rho_c \sim 5\rho_0$
- Studied in several ongoing and future experiments:
  - ✓ collider experiments: maximum phase space, minimally biased acceptance, free of target parasitic effects
  - ✓ fixed-target experiments: high rate of interactions, easily upgradeable, better vertex-finder for heavy flavor decays

# Multi-Purpose Detector

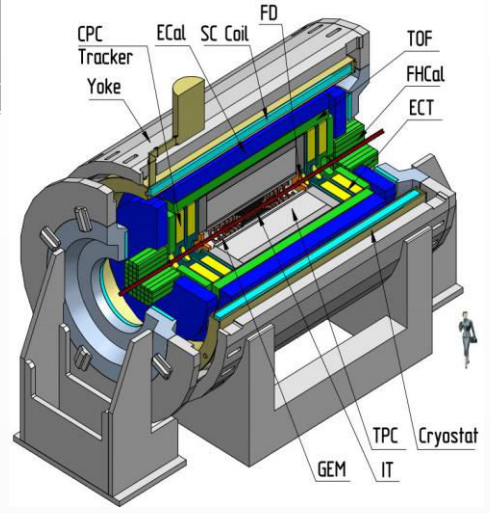
## Stage- I



Length	340 cm
Vessel outer radius	140 cm
Vessel inner radius	27 cm
Default magnetic field	0.5 T
Drift gas mixture	90% Ar+10% CH <sub>4</sub>
Maximum event rate	7 kHz ( $L = 10^{27} \text{ cm}^{-2}\text{s}^{-1}$ )



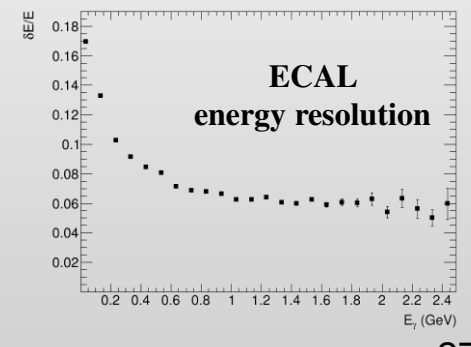
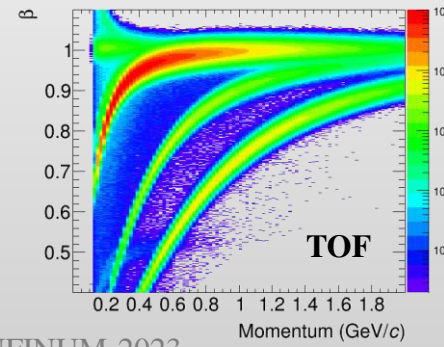
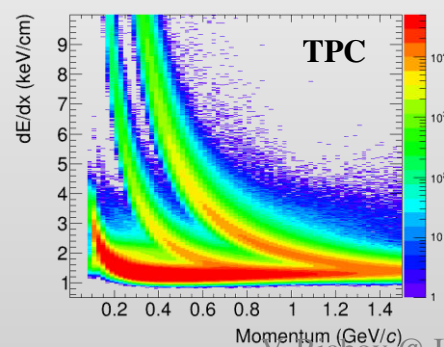
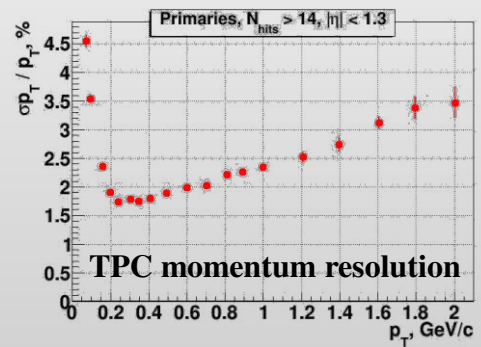
## Stage- II



- TPC:**  $|\Delta\phi| < 2\pi, |\eta| \leq 1.6$
- TOF, EMC:**  $|\Delta\phi| < 2\pi, |\eta| \leq 1.4$
- FFD:**  $|\Delta\phi| < 2\pi, 2.9 < |\eta| < 3.3$
- FHCAL:**  $|\Delta\phi| < 2\pi, 2 < |\eta| < 5$

- + ITS** (heavy-flavor measurements)
- + forward spectrometers**

Au+Au @ 11 GeV (UrQMD + full chain reconstruction)





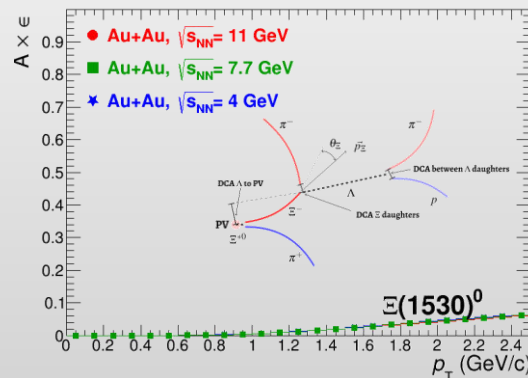
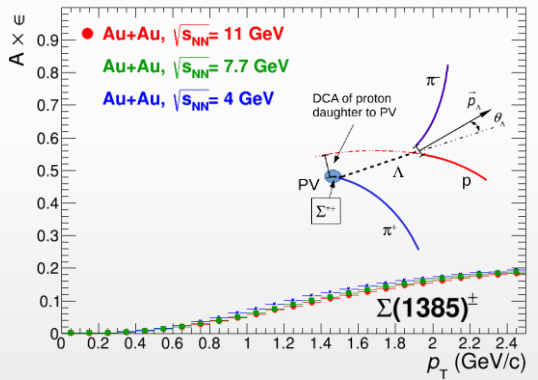
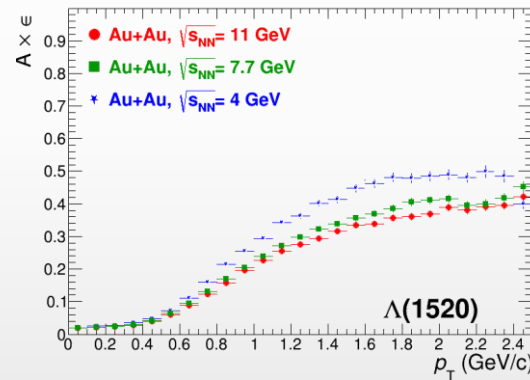
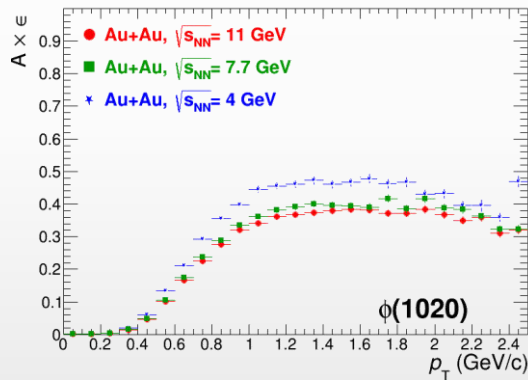
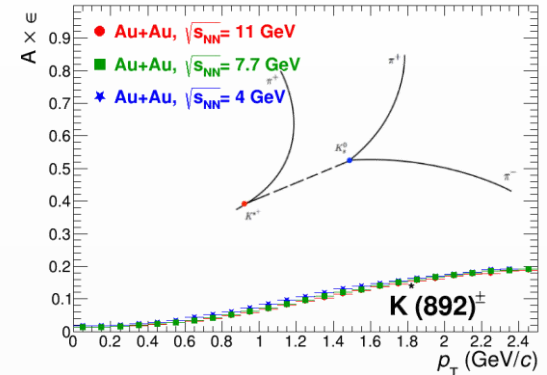
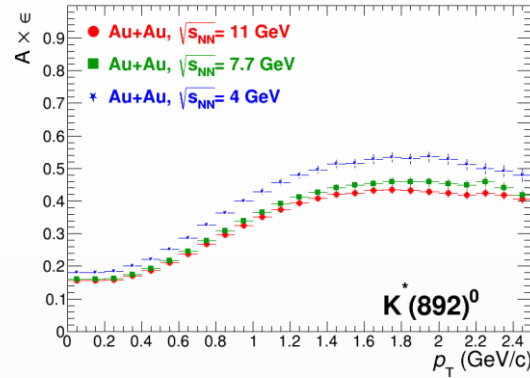
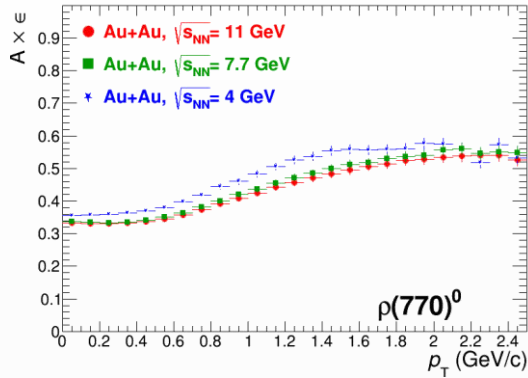
- ❖ 2022:
  - ✓ preparation of the SC magnet for cooling
- ❖ 2023:
  - ✓ cooling the magnet and MF measurement
  - ✓ installation of the support frame and detectors
- ❖ 2024:
  - ✓ MPD commissioning
  - ✓ first run with BiBi@9.2 GeV, ~ 50-100 M events for alignment, calibration and physics
- ❖ 2025 and beyond:
  - ✓ Au+Au @ 11 GeV, design luminosity
  - ✓ system size and collision energy scans

- Preparation of the MPD detector and experimental program is ongoing, all activities are continued
- All components of the MPD 1-st stage detector are in advanced state of production (subsystems, support frame, electronics platforms, LV/HV, control systems, cryogenics, cabling, etc.)

Schedule of the MPD-NICA is significantly affected by the current geopolitical situation (suspension of collaboration with CERN and Polish & Czech Republic member institutions, economical sanctions and problems with supplies of many components from western companies). The primary goal to have the MPD commissioned by the first beams at NICA collider is preserved.

# Reconstruction efficiencies

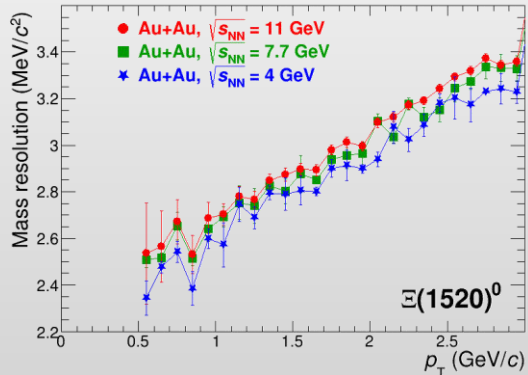
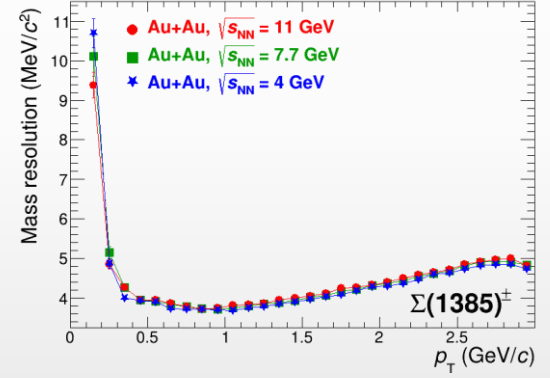
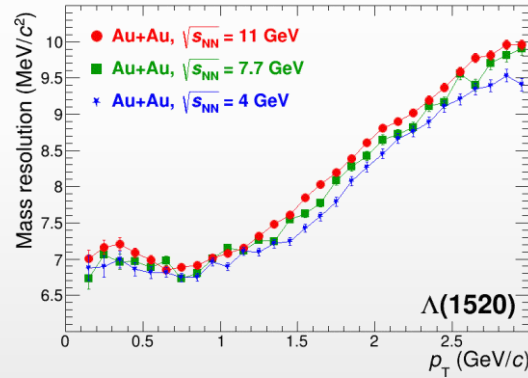
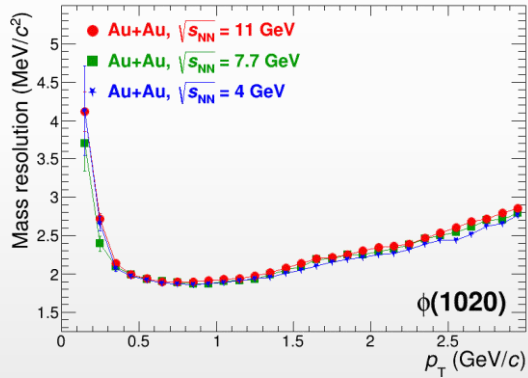
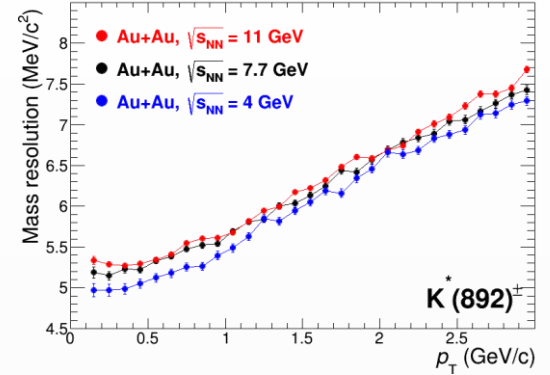
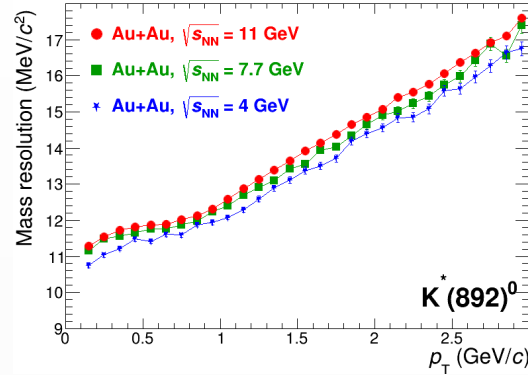
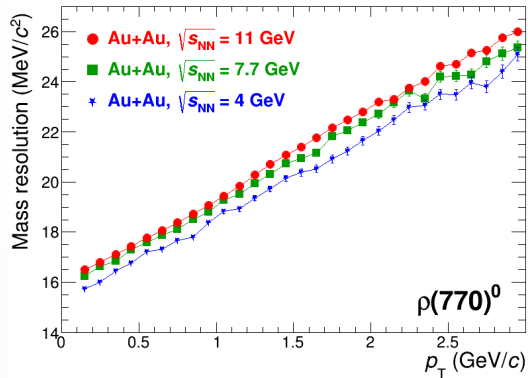
- Typical reconstruction efficiencies ( $A \times \epsilon$ ) in AuAu @ 4, 7.7 and 11 GeV,  $|y| < 1$



- Reasonable efficiencies in the wide  $p_T$  range,  $|y| < 1$
- Efficiencies are noticeably lower for multi-stage decays with weakly decaying daughters ( $\Xi$ ,  $\Lambda$ ,  $K_S^0$ )
- Measurements are possible from zero momentum
- Modest multiplicity (and/or  $\sqrt{s_{NN}}$ ) dependence

# Mass resolution:

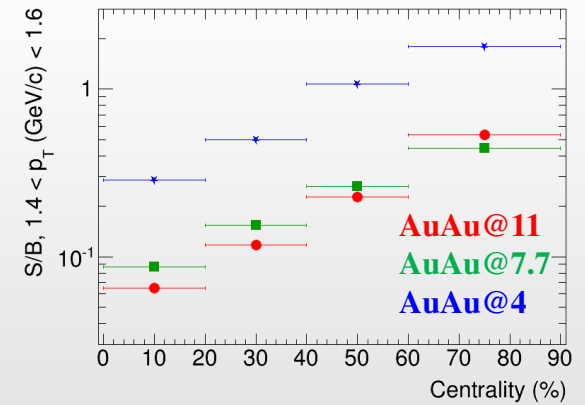
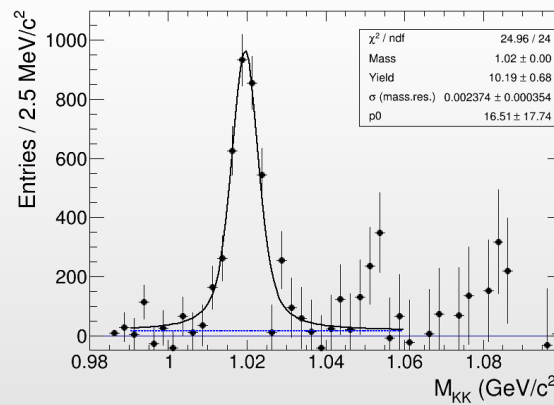
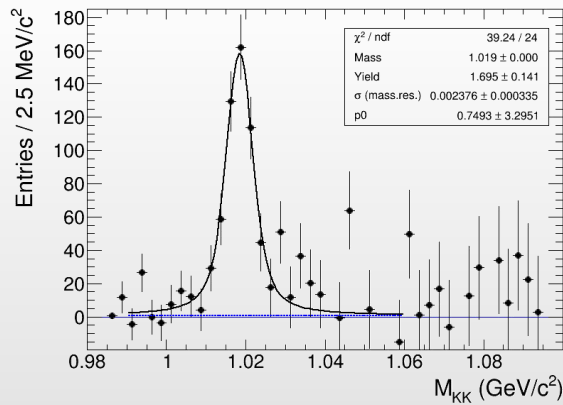
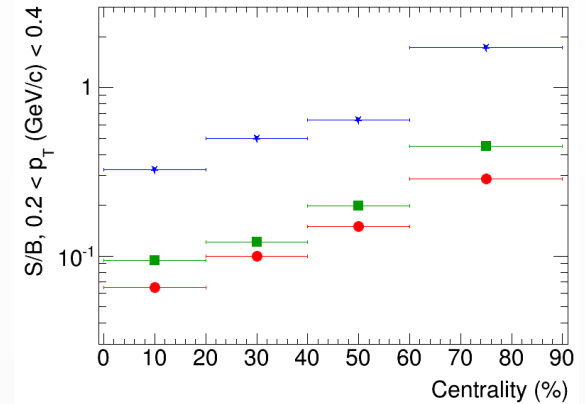
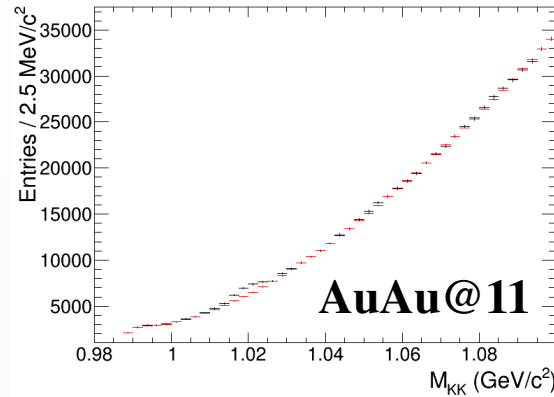
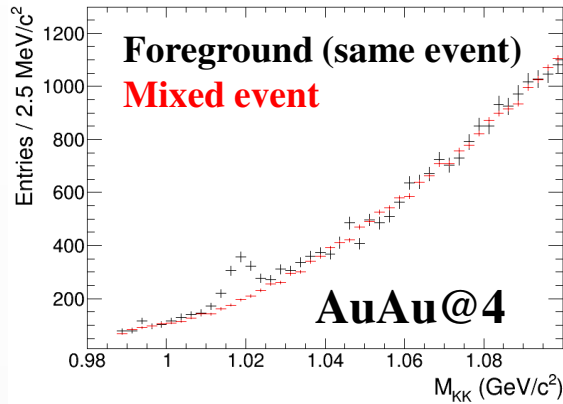
- Detector mass resolution ( $m_{\text{reconstructed}} - m_{\text{generated}}$ ) in AuAu @ 4, 7.7 and 11 GeV,  $|y| < 1$



- Mass resolution is good enough to preserve the capability for the line shape analysis
- Modest multiplicity (and/or  $\sqrt{s_{NN}}$ ) dependence

# $\phi(1020)$ , reconstructed peaks

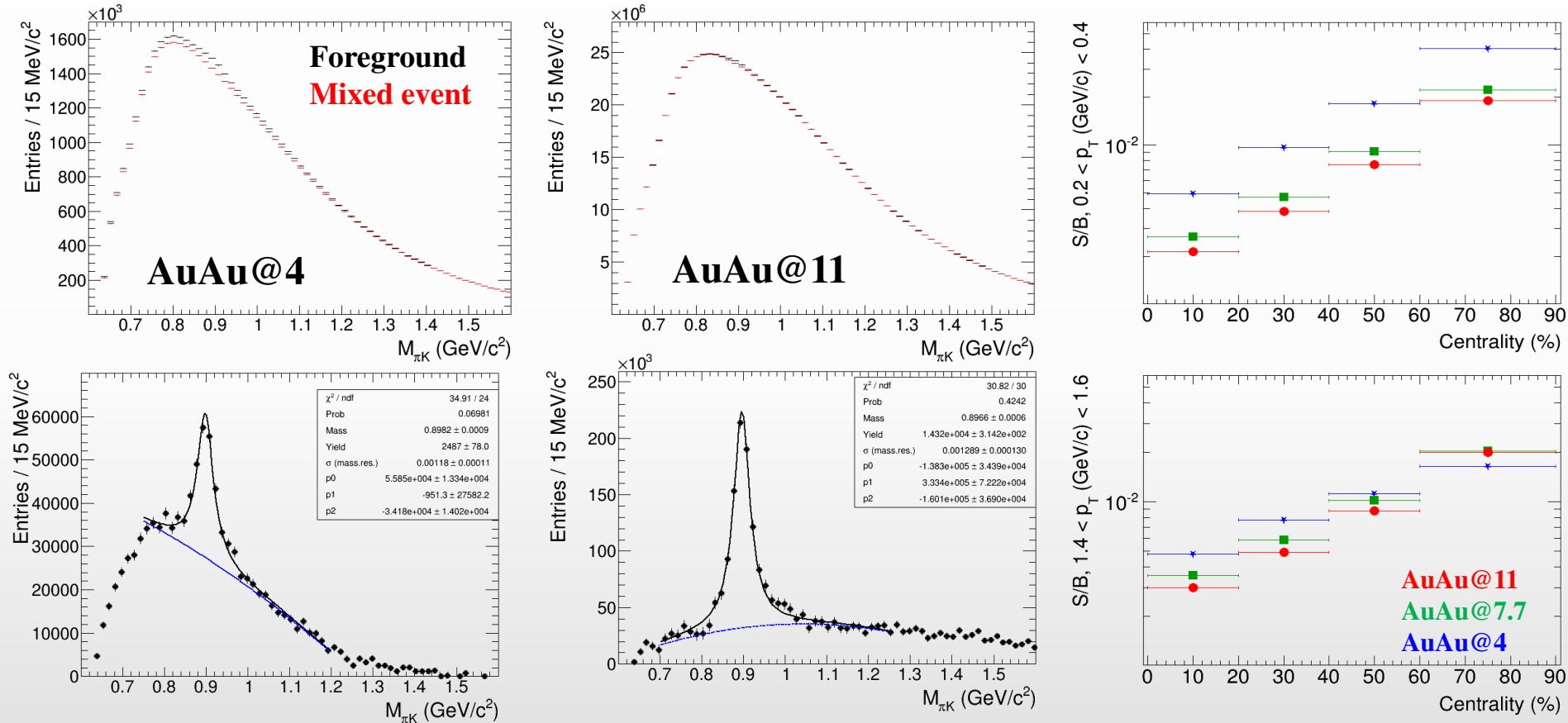
- UrQMD v.3.4: AuAu@11 (10M events), AuAu@7.7 (5M events), AuAu@4 (5M events)
- Full chain simulation and reconstruction,  $p_T = 0.2-0.4$  GeV/c,  $|y| < 1$



- Mixed-event combinatorial background is scaled to foreground at high mass and subtracted
- Distributions are fit to Voigtian function + polynomial
- Signal can be reconstructed at  $p_T > 0.2$  GeV/c, high- $p_T$  reach is limited by available statistics
- S/B ratios deteriorates with increasing centrality and collision energy

# $K^*(892)^0$ , reconstructed peaks

- UrQMD v.3.4: AuAu@11 (10M events), AuAu@7.7 (5M events), AuAu@4 (5M events)
- Full chain simulation and reconstruction,  $p_T = 0.2-0.4$  GeV/c,  $|y| < 1$



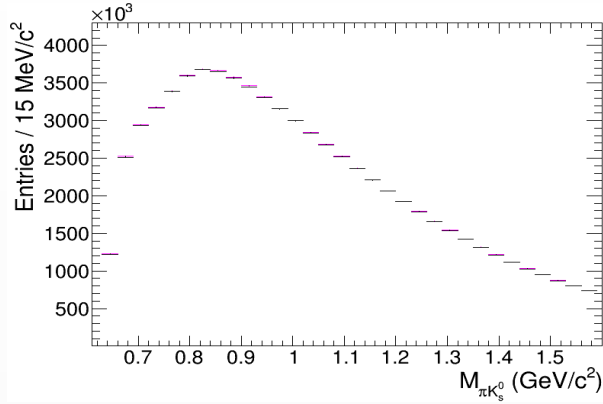
- Mixed-event combinatorial background is scaled to foreground at high mass and subtracted
- Distributions are fit to Voigtian function + polynomial
- Signal can be reconstructed at  $p_T > 0$  GeV/c, high- $p_T$  reach is limited by available statistics
- S/B ratios deteriorates with increasing centrality and collision energy



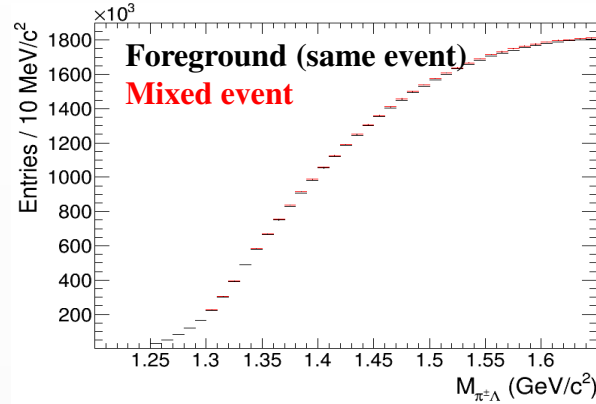
# $K^*(892)^\pm, \Sigma(1385)^\pm, \Xi(1530)^0$ , reconstructed peaks

- UrQMD v.3.4: AuAu@11 (10M events), full chain simulation and reconstruction,  $|y| < 1$

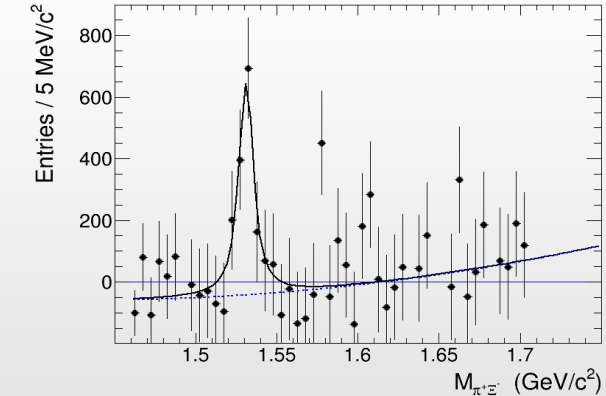
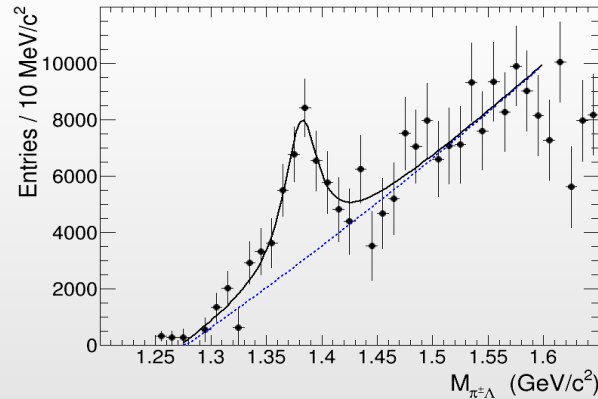
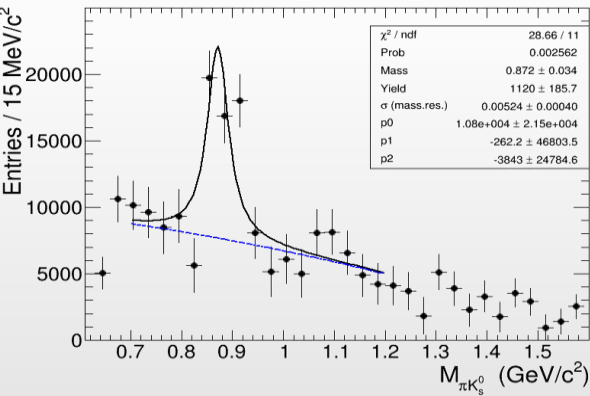
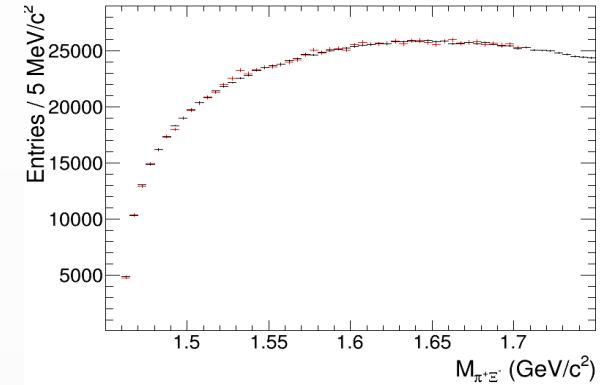
$K^{*\pm}, 0.2-0.4 \text{ GeV}/c$



$\Sigma(1385)^\pm, 0-0.5 \text{ GeV}/c$

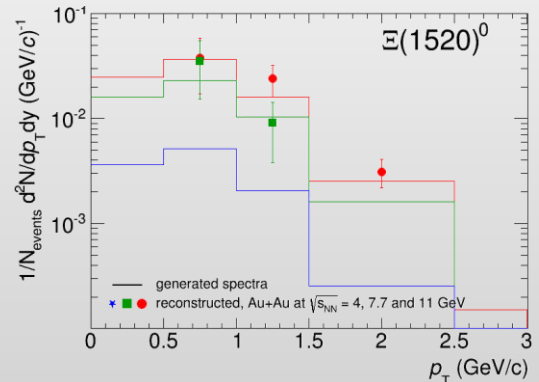
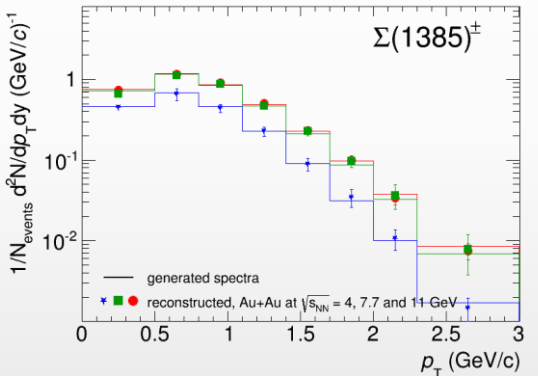
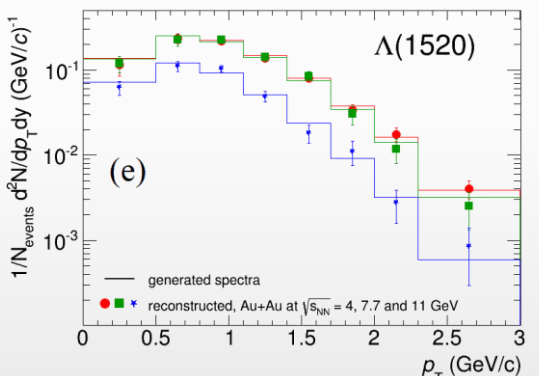
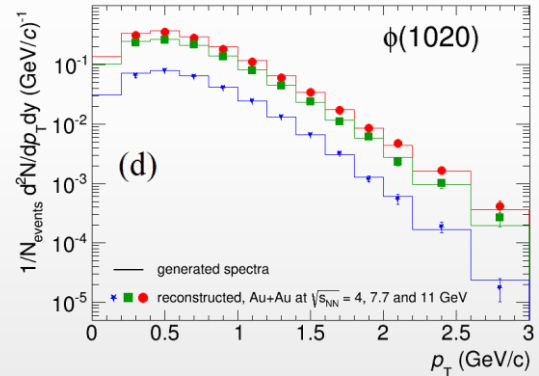
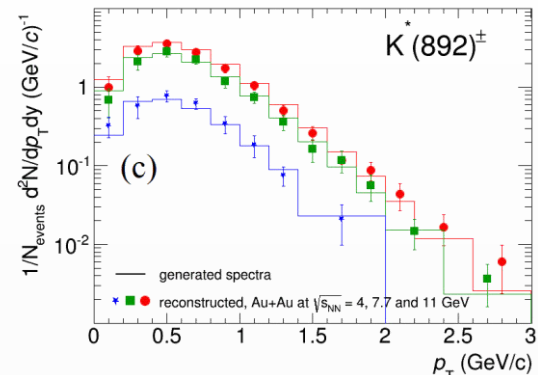
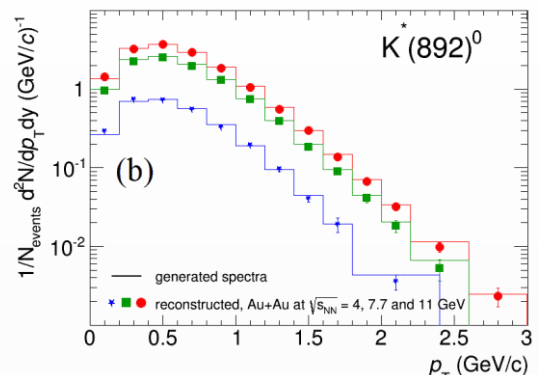
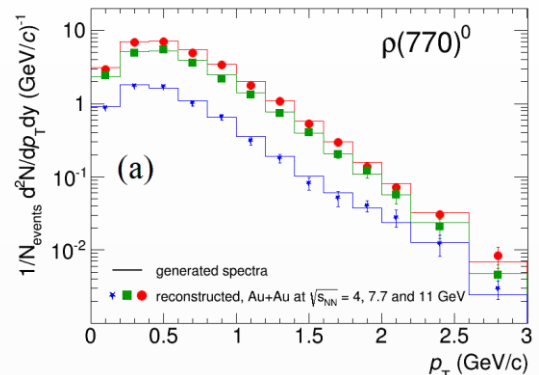


$\Xi(1530)^0, 0.5-1 \text{ GeV}/c$



- Can reconstruct signals for multistage decays of  $K^*(892)^\pm \rightarrow K_S^0 \pi^\pm$  ( $K_S^0 \rightarrow \pi^+ \pi^-$ ),  $\Sigma(1385)^\pm \rightarrow \pi^\pm \Lambda$  ( $\Lambda \rightarrow p \pi$ ) and  $\Xi(1530)^0 \rightarrow \pi^+ \Xi^-$  ( $\Xi^- \rightarrow \Lambda \pi^-$ , ( $\Lambda \rightarrow p \pi^-$ ))

- Full chain simulation and reconstruction,  $p_T$  ranges are limited by the possibility to extract signals,  $|y| < 1$



- Reconstructed spectra match the generated ones within uncertainties
- First measurements for resonances will be possible with accumulation of  $\sim 10^7$  A+A events
- Measurements are possible starting from  $\sim$  zero momentum  $\rightarrow$  sample most of the yield, sensitive to possible modifications
- Measurements of  $\Xi(1530)^0$  are very statistics hungry

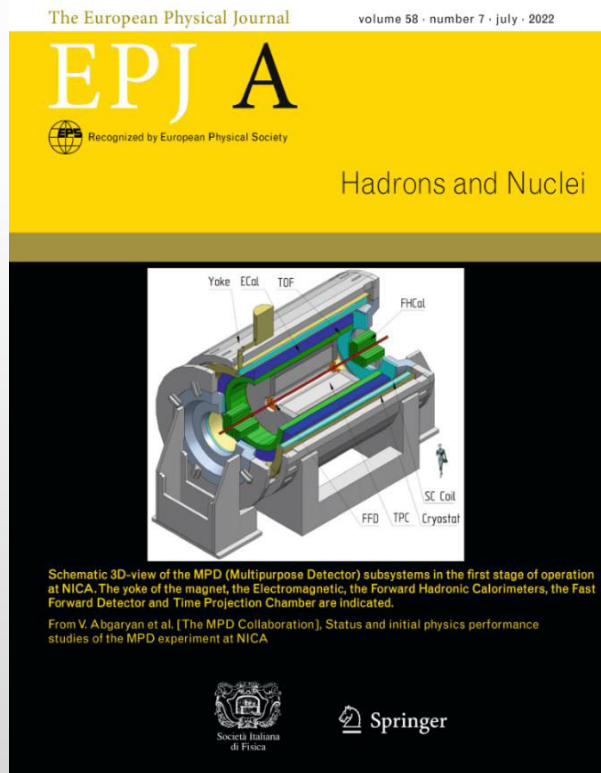
# Summary

- Measurement of resonances contribute to the MPD physical program
- Resonances are expected to be very sensitive to the properties of the partonic/hadronic medium produced in heavy-ion collisions at NICA energies
- First-look measurements for resonances with the MPD detector are possible in a wide  $p_T$  range from zero momentum up to  $\sim 3$  GeV/c with  $\sim 10^7$  sampled Au+Au collisions at  $\sqrt{s_{NN}} = 4-11$  GeV  $\rightarrow$  plausible for year-1 operation
- More detailed and multiplicity-dependent studies would require  $\times 10-50$  larger statistics, especially for multi-stage decays of  $K^*(892)^\pm$ ,  $\Sigma(1385)^\pm$  and  $\Xi(1520)^0$

# BACKUP

- ❖ Many ongoing construction works, theoretical and physics feasibility studies
- ❖ MPD publications: over 200 in total for hardware, software and physics studies (SPIRES)
- ❖ MPD @ conferences: presented at all major conferences in the field
- ❖ First collaboration paper recently published EPJA (~ 50 pages): Eur.Phys.J.A 58 (2022) 7, 140

## Status and initial physics performance studies of the MPD experiment at NICA



Eur. Phys. J. A manuscript No.  
 (will be inserted by the editor)

### Status and initial physics performance studies of the MPD experiment at NICA

The MPD Collaboration<sup>1</sup>

<sup>1</sup>The full list of Collaboration Members is provided at the end of the manuscript

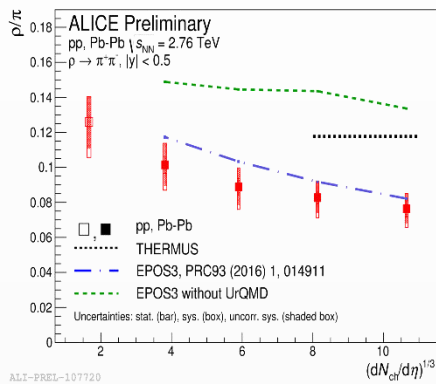
Received: April 20, 2022 / Accepted: date

1	<b>Abstract</b> The <b>Nucleon-based Ion Collider Facility</b>	22
2	<b>NICA</b> is under construction at the <b>Joint Institute for</b>	23
3	<b>Nuclear Research</b> (JINR), with commissioning of the	23
4	<b>facility</b> expected in late 2022. The <b>Multi-Purpose De-</b>	24
5	<b>tektor</b> (MPD) has been designed to operate at NICA	25
6	and its components are currently in production. The	25
7	detector is expected to be ready for data taking with	25
8	the first beams from NICA. This document provides	25
9	an overview of the landscape of the investigation of the	26
10	QCD phase diagram in the region of maximum bary-	26
11	onic density, where NICA and MPD will be able to	26
12	provide significant and unique input. It also provides	27
13	a detailed description of the MPD set-up, including its	27
14	various subsystems as well as its support and computing	28
15	infrastructures. Selected performance studies for partic-	29
16	ular physics measurements at MPD are presented and	31
17	discussed in the context of existing data and theoretical	33
18	expectations.	33
19	<b>Keywords</b> NICA - MPD - QCD	35
20		35
21	<b>Contents</b>	37
22	<b>1 Introduction</b>	37
23	<b>1.1 The Multi-Purpose Detector (MPD)</b>	37
24	<b>1.2 The NICA facility</b>	37
25	<b>1.3 The MPD detector</b>	37
26	<b>1.4 The MPD detector subsystems</b>	37
27	<b>1.5 The MPD detector subsystems</b>	37
28	<b>1.6 The MPD detector subsystems</b>	37
29	<b>1.7 The MPD detector subsystems</b>	37
30	<b>1.8 The MPD detector subsystems</b>	37
31	<b>1.9 The MPD detector subsystems</b>	37
32	<b>1.10 The MPD detector subsystems</b>	37
33	<b>1.11 The MPD detector subsystems</b>	37
34	<b>1.12 The MPD detector subsystems</b>	37
35	<b>1.13 The MPD detector subsystems</b>	37
36	<b>1.14 The MPD detector subsystems</b>	37
37	<b>1.15 The MPD detector subsystems</b>	37
38	<b>1.16 The MPD detector subsystems</b>	37
39	<b>1.17 The MPD detector subsystems</b>	37
40	<b>1.18 The MPD detector subsystems</b>	37
41	<b>1.19 The MPD detector subsystems</b>	37
42	<b>1.20 The MPD detector subsystems</b>	37
43	<b>1.21 The MPD detector subsystems</b>	37
44	<b>1.22 The MPD detector subsystems</b>	37
45	<b>1.23 The MPD detector subsystems</b>	37
46	<b>1.24 The MPD detector subsystems</b>	37
47	<b>1.25 The MPD detector subsystems</b>	37
48	<b>1.26 The MPD detector subsystems</b>	37
49	<b>1.27 The MPD detector subsystems</b>	37
50	<b>1.28 The MPD detector subsystems</b>	37
51	<b>1.29 The MPD detector subsystems</b>	37
52	<b>1.30 The MPD detector subsystems</b>	37
53	<b>1.31 The MPD detector subsystems</b>	37
54	<b>1.32 The MPD detector subsystems</b>	37
55	<b>1.33 The MPD detector subsystems</b>	37
56	<b>1.34 The MPD detector subsystems</b>	37
57	<b>1.35 The MPD detector subsystems</b>	37
58	<b>1.36 The MPD detector subsystems</b>	37
59	<b>1.37 The MPD detector subsystems</b>	37
60	<b>1.38 The MPD detector subsystems</b>	37
61	<b>1.39 The MPD detector subsystems</b>	37
62	<b>1.40 The MPD detector subsystems</b>	37
63	<b>1.41 The MPD detector subsystems</b>	37
64	<b>1.42 The MPD detector subsystems</b>	37
65	<b>1.43 The MPD detector subsystems</b>	37
66	<b>1.44 The MPD detector subsystems</b>	37
67	<b>1.45 The MPD detector subsystems</b>	37
68	<b>1.46 The MPD detector subsystems</b>	37
69	<b>1.47 The MPD detector subsystems</b>	37
70	<b>1.48 The MPD detector subsystems</b>	37
71	<b>1.49 The MPD detector subsystems</b>	37
72	<b>1.50 The MPD detector subsystems</b>	37
73	<b>1.51 The MPD detector subsystems</b>	37
74	<b>1.52 The MPD detector subsystems</b>	37
75	<b>1.53 The MPD detector subsystems</b>	37
76	<b>1.54 The MPD detector subsystems</b>	37
77	<b>1.55 The MPD detector subsystems</b>	37
78	<b>1.56 The MPD detector subsystems</b>	37
79	<b>1.57 The MPD detector subsystems</b>	37
80	<b>1.58 The MPD detector subsystems</b>	37
81	<b>1.59 The MPD detector subsystems</b>	37
82	<b>1.60 The MPD detector subsystems</b>	37
83	<b>1.61 The MPD detector subsystems</b>	37
84	<b>1.62 The MPD detector subsystems</b>	37
85	<b>1.63 The MPD detector subsystems</b>	37
86	<b>1.64 The MPD detector subsystems</b>	37
87	<b>1.65 The MPD detector subsystems</b>	37
88	<b>1.66 The MPD detector subsystems</b>	37
89	<b>1.67 The MPD detector subsystems</b>	37
90	<b>1.68 The MPD detector subsystems</b>	37
91	<b>1.69 The MPD detector subsystems</b>	37
92	<b>1.70 The MPD detector subsystems</b>	37
93	<b>1.71 The MPD detector subsystems</b>	37
94	<b>1.72 The MPD detector subsystems</b>	37
95	<b>1.73 The MPD detector subsystems</b>	37
96	<b>1.74 The MPD detector subsystems</b>	37
97	<b>1.75 The MPD detector subsystems</b>	37
98	<b>1.76 The MPD detector subsystems</b>	37
99	<b>1.77 The MPD detector subsystems</b>	37
100	<b>1.78 The MPD detector subsystems</b>	37

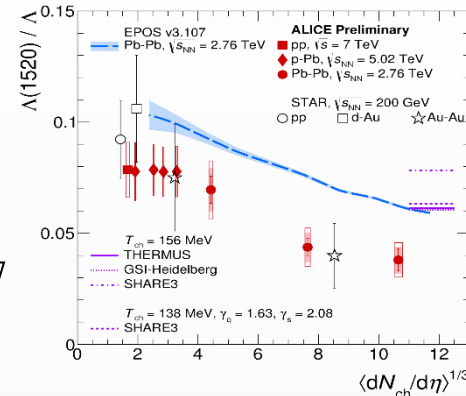
# Experimental results, A+A at $\sqrt{s_{NN}} = 200\text{-}5000$ GeV

increasing lifetime  $\longrightarrow$

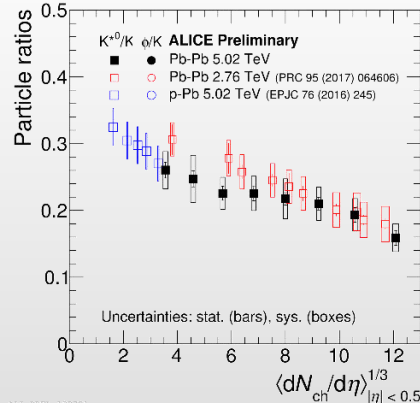
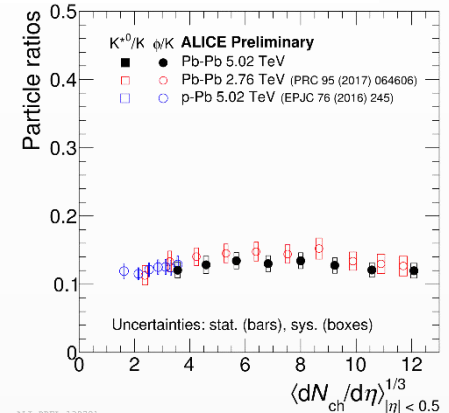
	$\rho(770)$	$K^*(892)$	$\Lambda(1520)$	$\Xi(1530)$	$\phi(1020)$
$c\tau$ (fm/c)	1.3	4.2	12.7	21.7	46.2
$\sigma_{\text{rescatt}}$	$\sigma_{\pi}\sigma_{\pi}$	$\sigma_{\pi}\sigma_K$	$\sigma_K\sigma_p$	$\sigma_{\pi}\sigma_{\Xi}$	$\sigma_K\sigma_K$



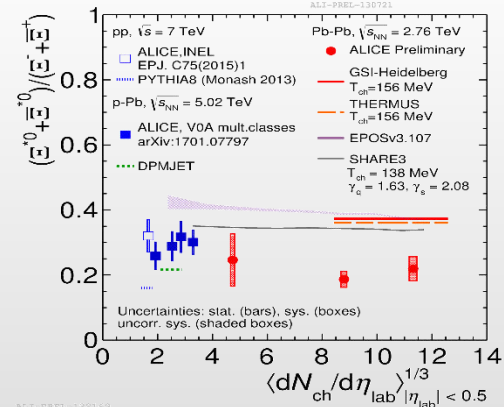
ALI-PREL-107720



ALI-PREL-129193



ALI-PREL-108941

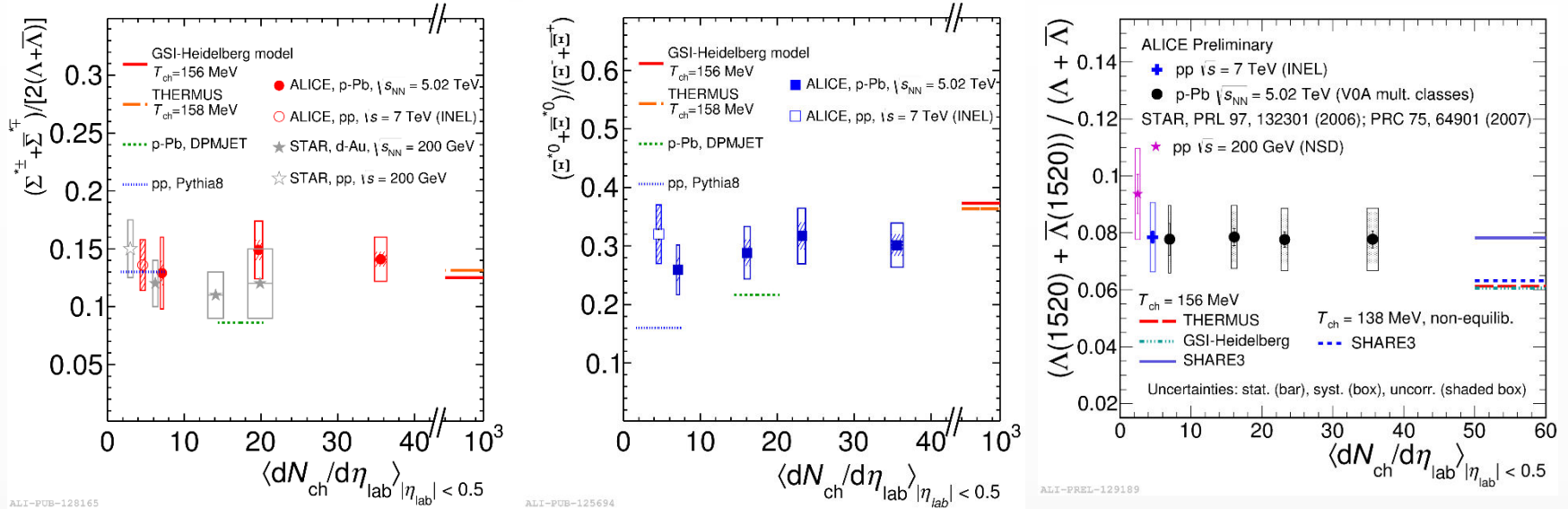


ALI-PREL-120162

- Suppressed production of short-lived resonances ( $\tau < 20$  fm/c) in central A+A collisions  $\rightarrow$  rescattering takes over the regeneration
- No modification is observed for  $\phi$ -meson ( $\tau \sim 40$  fm/c)  $\rightarrow$  behaves like a stable particle

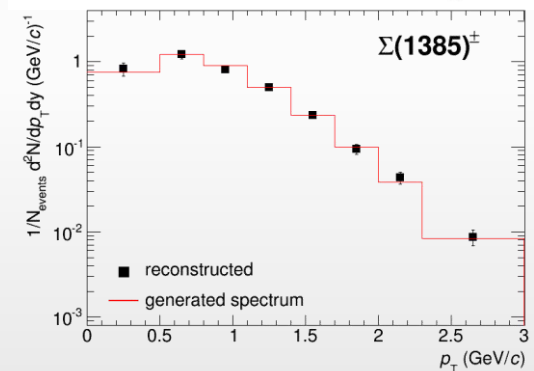
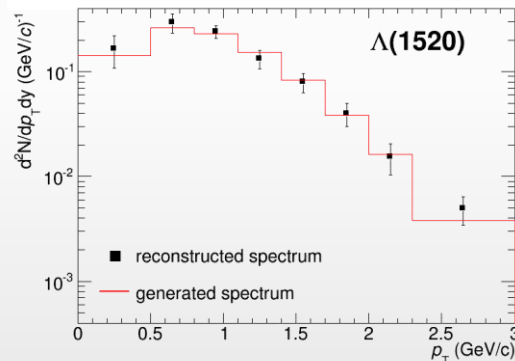
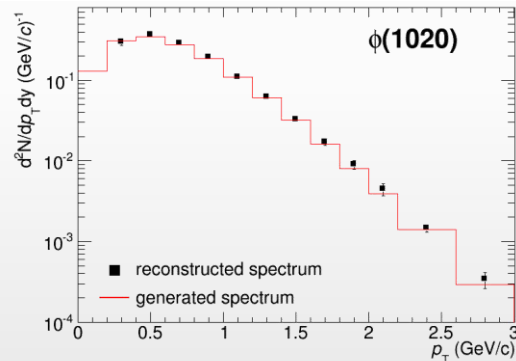
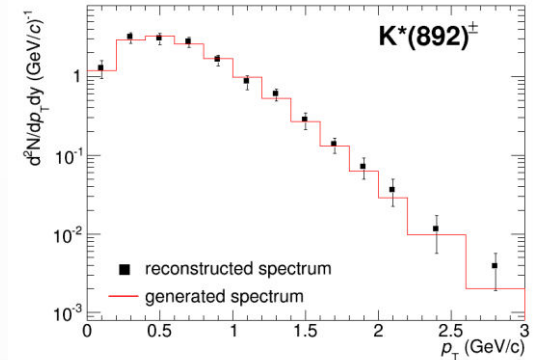
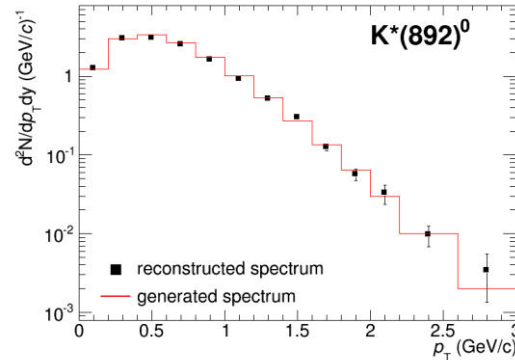
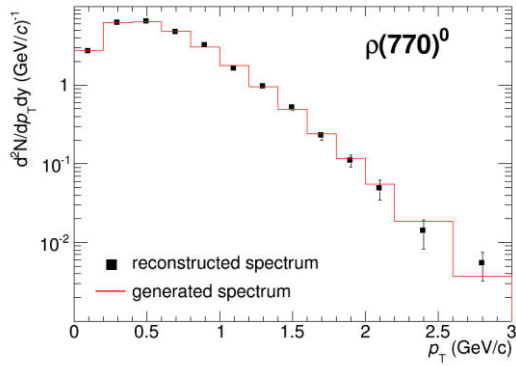
# Enhanced strangeness production, resonances

EPJ C77 (2017) 389



- Ratios of resonances to stable particles with the same strangeness do not depend on multiplicity in pp and p-Pb  $\rightarrow$  confirms that strangeness enhancement depends predominantly on the strangeness content, rather than on the particle mass
- Ratios do not show strong dependence on collision energy,  $\sqrt{s} = 0.2-5.02$  TeV
- No model reproduces all measurements simultaneously

❖ Full chain simulation and reconstruction,  $p_T$  ranges are limited by the possibility to extract signals,  $|y| < 1$



- ❖ Reconstructed spectra match the generated ones within uncertainties
- ❖ First measurements for resonances will be possible with accumulation of  $\sim 10^7$  Bi+Bi events
- ❖ Measurements are possible starting from  $\sim$  zero momentum  $\rightarrow$  sample most of the yield
- ❖ Measurements of  $\Xi(1530)^0$  are very statistics hungry